Microplastics and suspended particles in a strongly impacted coastal environment: Composition, abundance, surface texture, and interaction with metal ions

A.D. Forero López, D.M. Truchet, G.N. Rimondino, L. Maisano, C.V. Spetter, N.S. Buzzi, M.S. Nazzarro, F.E. Malanca, O. Furlong, M.D. Fernández Severini

PII: S0048-9697(20)35942-8

DOI: https://doi.org/10.1016/j.scitotenv.2020.142413

Reference: STOTEN 142413

To appear in: *Science of the Total Environment*

Received date: 10 August 2020

Revised date: 14 September 2020

Accepted date: 14 September 2020

Please cite this article as: A.D.F. López, D.M. Truchet, G.N. Rimondino, et al., Microplastics and suspended particles in a strongly impacted coastal environment: Composition, abundance, surface texture, and interaction with metal ions, *Science of the Total Environment* (2020), https://doi.org/10.1016/j.scitotenv.2020.142413

MICROPLASTICS AND SUSPENDED PARTICLES IN A STRONGLY IMPACTED COASTAL ENVIRONMENT: COMPOSITION, ABUNDANCE, SURFACE TEXTURE, AND INTERACTION WITH METAL IONS.

A.D. Forero López[1*], D.M. Truchet[1,2], G.N. Rimondino[3], L. Maisano[1,4], C.V. Spetter[1,5], N.S. Buzzi[1,2], M.S. Nazzarro[6], F.E. Malanca[3], O. Furlong[6], M.D. Fernández Severini[1*].

1: Instituto Argentino de Oceanografía (IADO), CONICET/UNS, CCT-Bahía Blanca, Camino La Carrindanga, km 7.5, Edificio E1, B8000FWB, Bahía Blanca, Buenos Aires, Argentina.

2: Departamento de Biología, Bioquímica y Farmacia, Universidad Nacional del Sur (UNS), San Juan 670, B8000ICN, Bahía Blanca, Buenos Aires, Argentina.

3: Instituto de Investigaciones en Fisicoquímica de Córdoba (INFIQC), Departamento de Fisicoquímica, Facultad de Ciencias Químicas. Universidad Nacional de Córdoba, Ciudad Universitaria X5000HUA, Córdoba, Argentina.

4: Departamento de Geología, Universidad Nacional del Sur (UNS), San Juan 670, B8000ICN, Bahía Blanca, Buenos Aires, Argentina

5: Departamento de Química, Universidad Nacional del Sur (UNS), Avenida Alem 1253, B8000CPB, Bahía Blanca, Buenos Aires, Argentina.

6: Instituto de Física Aplicada (INFAP), Departamento de Física, CONICET-Universidad Nacional de San Luis, Av. Ejército de los Andes 950, 5700, San Luis, Argentina.

* *Corresponding authors at: Instituto Argentino de Oceanografía (IADO), CONICET/UNS, CCT-BB Camino La Carrindanga, km 7.5, Edificio E1, B8000FWB, Bahía Blanca, Pcia. de Bs. As., Argentina. E- mail address: (aforero@iado-conicet.gob.ar;A.D. Forero López; melisafs@criba.edu.ar ;M.D. Fernádez Severini).*

Highlights

- First detailed assessment of suspended particulate matter (SPM) and microplastics (MPs) in the Bahía Blanca Estuary.
- Metal-phosphates bonds and mixtures of Fe^{3+}/Fe^{2+} were detected in the SPM.
- Cr, Ni, Fe, Cd, Zn, Pb, and Mn were detected in the SPM
- MPs abundance ranged 3 to 11.5 items.L^{-1}
- MPs were mostly represented by semi-synthetic cellulose fibers and poly(amide)
- SPM and MPs as the main transport vectors for metals in the Bahía Blanca Estuary.

Abstract

The composition and the interaction of the suspended particulate matter (SPM) with metal ions, along with the presence and characteristics of microplastics, were analyzed for the first time in the water column of the inner zone of Bahía Blanca Estuary during winter (June, July, and August) 2019. Surface analysis techniques (Scanning Electron Microscopy combined with Energy Dispersive X-Ray Spectroscopy, X-Ray Photoelectron Spectroscopy, and X-Ray Diffraction) were employed to obtain an in-depth characterization of the particulate matter, suggesting the presence of Fe in our samples, with a mixture of Fe^{3+}/Fe^{2+} oxidation states. Microplastics ranged in concentrations between 3 and 11.5 items L^{-1}, with an average of 6.50 items L^{-1}

(S.E:±4.01), being fibers the most abundant type. Infrared Spectroscopy suggests that these fibers correspond to semi-synthetic cellulose-based and poly(amide) remains. We concluded that the SPM is a significant vehicle for metals which might have adverse effects on marine organisms.

Keywords: Microplastics; Suspended particulate matter; Metal ions; Biogeochemistry, Bahía Blanca Estuary.

1. Introduction

Currently, microplastics (MPs) represent a potential danger for terrestrial and aquatic ecosystems, as well as for air quality since, unlike other materials, these pollutants are resistant to degradation (Yu et al., 2019). They are defined as plastic debris (fibers, fragments, pellets, or particles) with a size of less than 5 mm (GESAMP, 2015; Guo and Wang, 2019), and they can be present in the environment as primary or secondary microplastics. Primary MPs are released directly into the environment as small particles generated from industrial and cosmetic products, textiles, and medicines. The secondary ones are small plastic fragments progressively generated by the continuous weathering of plastic litter (Silva et al., 2018). In marine aquatic environments, MPs are ubiquitous, and they can be found in the water column associated with suspended particulate matter (SPM), and in marine sediments, as well as in the biota (Leslie et al., 2011; Lambert and Wagner, 2018). On the one hand, and due to their small size, they can be ingested directly by diverse organisms, such as polychaetes (Wright et al., 2013), zooplankton (Sun et al., 2018), oysters (Fernández Severini et al., 2019), crabs (Villagran et al., 2020), and fish (Vendel et al., 2017), among others. In some of these organisms, the ingestion of MPs has been linked to their health status, body condition, oxidative damage, neurotoxicity, starvation, and

alterations in their reproductive biology (Von Moss et al., 2012; Wright et al., 2013; Anbumani and Kakkar, 2018; Critchell and Hoogenboom, 2018). Another concern about MPs is their association with toxic chemicals, as they tend to adsorb and accumulate chemical pollutants, such as heavy metals and hydrophobic/hydrophilic organic compounds, which are also present in marine environments (Silva et al., 2018; Guo and Wang, 2019; Yu et al., 2019) and could be ingested by organisms. Also, the adsorption of metal ions on the polymer surface is increased as the material ages, along with its polarity, surface area, and porosity (Ashton et al., 2010). Furthermore, MPs also serve as substrate and/or vector for the widespread distribution of potential pathogens such as microorganism colonies that could infect biotic species or alter pristine places (Zettler et al., 2013).

Estuaries are coastal environments where the chemical, biological, and physical processes are highly dynamic, and they act as "filters" or "reactors" that transport inputs from rivers to oceans (Cochran, 2014). In these environments, the SPM is based on seston and sediments, which are either temporary or permanent particles, always in exchange with the reservoir of seabed sediments and the intertidal flats (Turner and Millward, 2002; Guinder et al., 2010; Souza Machado et al., 2015). Moreover, the biological and chemical composition of the SPM is strongly influenced by weather conditions, seasons, and the input of nutrients (Shang and Xu, 2018). In marine environments, SPM comes from continental and coastal erosion, rivers, anthropogenic activities, chemical-biological processes *in situ*, and the atmosphere (Turner and Millward, 2002). The SPM is an important parameter that influences the primary and secondary production of plankton, as well as the concentration of different organic and inorganic trace elements in the aquatic environment (Meybeck et al., 2004; Håkanson, 2006; Shang and Xu, 2018).

The study area, the Bahía Blanca Estuary (hereafter, BBE, **Figure 1**) is a highly productive marine ecosystem, considered as one of the most significant coastal environments in the southwestern Atlantic due to both, the high chlorophyll-*a* and nutrient concentrations (Guinder et al., 2012; Spetter et al., 2015a). However, the BBE is affected by different anthropogenic activities, such as the presence of important urban, industrial, and harbor areas (Marcovecchio et al., 2008; Fernández Severini et al., 2011), especially on the northern boundary of the Principal Channel (Canal Principal), where populated areas as Bahía Blanca (300k inhabitants), Punta Alta (58k inhabitants), Ingeniero White (10k inhabitants), and General Daniel Cerri (9k inhabitants) are located. Also, one of the largest petrochemical complexes in South America is situated on the northern shore, with oil refineries, petrochemical industries, and textiles plants that discharge their effluents into the estuary (Arias et al., 2010). Furthermore, the most extensive naval base (Puerto Belgrano) and the largest deep port (Puerto Galván) of Argentina are also located in the BBE which is regularly navigated by large navy ships, small-scale fishing boats, oil tankers as well as by large cargo ships that require regular dredging of the Principal Channel (Fernández Severini et al., 2012; Truchet et al., 2019; Fernández Severini et al., 2019).

A high number of analytical techniques can be used to obtain accurate information on the SPM, and MPs. X-Ray Photoelectron Spectroscopy (XPS) is a highly surface-sensitive technique used for compositional and chemical state analyses. It gives information about the outer surface of particles, and also about the particle source. It also reveals the identification and relative concentration of elements and compounds, including the chemical and electronic states of their core-ionized atoms (Galvao et al., 2018). XPS is a non-destructive technique that requires no sample handling and has been used to identify (and/or quantify) light elements. The surface

characterization of the mineralogical phases of the SPM individual particles, as well as the metals associated with MPs and the degree of weathering, can be analyzed through Scanning Electron Microscopy combined with Energy Dispersive X-Ray Spectroscopy (SEM/EDX). Thus, providing combined information about the physical, morphological, and chemical properties of solid-phase particles (Galvao et al., 2018). X-Ray Diffraction (XRD) is another surface analysis technique to investigate the chemical structure of a shallow layer in solid surfaces in the order of a few nanometers. It is based on the principle that different crystalline structures in solid-state materials diffract X-rays in different directions and intensities, allowing the identification of their crystal structure (Cienfuegos and Vaitsman, 2000). Infrared Spectroscopy (FT-IR) is a powerful and non-invasive tool for determining the chemical composition of MPs, identifying the different vibrational modes of the functional groups present in the polymer matrix. The application of spectroscopic methods, such as FT-IR to MPs, allows its chemical characterization and the discrimination of plastic particles from natural ones.

To the best of our knowledge, there is no data available of these types of studies with a detailed characterization of MPs and SPM, including different surface analysis techniques, in none of the coastal areas of the Southwestern Atlantic Ocean. Moreover, there are just a few studies around the world that have analyzed the combined behavior and dynamics of the MPs and SPM, and their effects on the marine biota (Wang et al., 2017; Frère et al. 2018; Ogonowski et al., 2018; Atwood et al., 2019; Harris et al., 2019). Thus, the main objectives of the present study were: i) Characterize the particles present in the SPM in the water column at Cuatreros Port (BBE, southwest of the Province of Buenos Aires, Argentina); ii) Identify, characterize, and quantify MPs in the water column; iii) Assess the role of SPM in the transport of pollutants, such as MPs

and heavy metals; and iv) Relate the information about MPs to their interaction with heavy metals.

Materials and methods

2.1 Study Area

The BBE is a mesotidal system (38°55.5′10.52" S; 62°03′20.75" W) situated in the Southwestern Atlantic Ocean in Buenos Aires province (Argentina), where semidiurnal tides are predominant, and the average tidal amplitude is 2.5 and 3.4 m during the neap and spring tides, respectively. It extends over 2,300 km^2 and is formed by a series of small channels running with an NW-SE orientation, separated by extensive tidal flats (Perillo et al., 2001). It is characterized by a dry temperate climate with low precipitation and high evaporation rates. The mean annual temperature is 15.6 °C and ranges from 22.7 °C to 8.1°C in the Austral summer and winter, respectively. The mean annual precipitation is 460 mm, and the predominant wind direction is from the NNW (mean velocity: 22.5 $km\ h^{-1}$) (Piccolo and Diez, 2004). Salinity ranges from 25.7 to 37.1 PSU with temporal variations, presenting higher values in late spring and summer (Fernández-Severini et al., 2012). In the tidal flats, sediments range from fine sand to mud, although siliciclastic grains are predominantly composed of quartz, feldspar, heavy minerals, and organic matter (Cuadrado and Pizani, 2007; Spetter et al., 2015b).Furthermore, the BBE is a crucial productive marine ecosystem in Argentina and South America, due to its phytoplankton density with a high nutrient concentration (Freije et al., 2008; Spetter et al., 2015a).

In the current study, the sampling site was located in the innermost area of the estuary at Cuatreros Port (CP) (38º45’00’’S; 62º22’46’’ W). This area has a mean depth of 7 m, with vertically homogeneous chemical conditions in the water column that

maintain significant amounts of SPM, but with high turbidity because of the combined effect of winds and tidal currents (Perillo et al., 2001; Gélos et al., 2004). The area presents the highest primary production of the system (Guinder et al., 2015), with chlorophyll-*a* concentrations over 40 mg L^{-1} (Freije and Marcovecchio, 2004). This area also receives sewage discharge inputs from the "Tercera Cuenca" Treatment Plant, and local untreated domestic wastes. Other water contributions to the estuary are the small freshwater tributaries, Sauce Chico, Aguará, Saladillo de García and Napostá that also receive pollutants mainly from different agricultural and livestock activities (Marcovecchio, 2000; Limbozzi and Leitao, 2008; Puzzi and Marcovecchio, 2018) (**Figure 1**).

2.2 Field sampling

Four surface water (0.5-1 m) samplings were carried out during the 2019 southern hemisphere winter (June, July, and August) at CP. A total of 7 surface samples of the water column were taken manually with conditioned 1.5 L glass bottles (n=7, three replicates each) for the SPM analysis, and the same procedure was followed for the MPs samples. The physicochemical parameters [dissolved oxygen (DO), temperature (T°), salinity, pH, and turbidity] were measured at 1 m depth with a multisensor HANNA Hi9828. For the characterization of chlorophyll-*a* (Chl-*a*), a total of 4 samples with three replicates each were collected in plastic bottles. All the samples were immediately transported to the laboratory for their corresponding analyses in refrigerated boxes.

2.3 *Chl-a analysis*

Water samples were filtered through glass microfiber filters grade F (0.70 µm). The material retained in the filter was frozen (-20 °C) in the dark and in aluminum foil

envelopes. Then, Chl-*a* concentration (µg L^{-1}) was determined spectrophotometrically using a Jenway 6715 UV-Vis spectrophotometer and following the methodology proposed by APHA (1998).

2.4 SPM recovery

Water samples were vacuum-filtered through nitrocellulose filters (0.45 µm pore size, Millipore) and then, the filters with the sample were dried at 50 (± 5) °C to constant weight. The SPM samples were weighed on an analytical balance and stored in a desiccator until further analysis. The SPM concentration was expressed as the mean $mg.L^{-1}$ (± S.E).

2.5 Analytical Methods

Heavy metal content was determined by ICP-OES using a Shimadzu Multitype ICPE-9000 Spectrometer. Samples were previously digested with 6 mL of HNO3: HClO4 mixture (5:1 v/v) at 110 (±10) °C in a CEM MARS 6 microwave, under a close system. Then, the volume was adjusted to 10 mL with HNO_3 0.7 %. In all cases, international protocols of cleaning procedures were taken into account (APHA, 1998) to avoid heavy metal contamination. The method detection limit (MDL) was calculated for each metal by multiplying the standard deviation of 20 blank replicates by the Student's t-test at the 99% confidence level (at n − 1 degrees of freedom) (Federal Register, 1984; EPA, 2016), resulting in the following values (µg g -1): Cd 0.034, Cr 0.05, Cu 0.09, Fe 3, Mn 0.23, Ni 0.05, Pb 0.04 and Zn 0.011.

The mineralogical composition of the SPM was determined by XRD in a Rigaku D-Max III-C diffractometer with CuKα radiation and a graphite monochromator, working at 35 kV and 15 mA, between 3 and 70° 2θ (steps of 0.04° 2θ and 1 s counting

time per step) and using quartz and alumina as an internal standard. SEM-EDX surface analyses of previously gold-coated samples were performed with a Zeiss Evo Ma10. The microscope was operated at 20 Kv in a working distance of 8-9 mm. The size distribution of non-organic grain was performed in a Malvern Mastersizer 2000, using a pre-treated sample that was incubated with H_2O_2 30 % initially at room temperature and then at 60°C, until removing all the organic matter.

In order to examine the chemical state of the elements present on the surface of the particles of the remaining SPM samples, they were treated with H_2O_2 30% at 60º for 5 h. The samples were analyzed using a VG Microtech ESCA spectrometer with a non-monochromatic Al Kα radiation source (300 W, 14 kV, hν = 1486.6 eV), combined with a VG-100-AX hemispherical analyzer operating at 25 eV pass energy. All the XPS spectra were calibrated with reference to the adventitious C1s peak at 284.8 eV to rule out any possible spectral shift due to a charging effect. The chamber pressure was kept at <10−9 torr during the measurements. All the XPS spectra were deconvoluted using Casas XPS software with a Gaussian–Lorentzian mix function.

2.6 Cleaning procedure for detection of MPs in SPM

In order to prevent contamination from MPs airborne, all the materials used for the sampling, filtration, and analyses in the laboratory were rinsed with deionized or ultra-pure water (Milli Q water quality), ethanol (70 %) and then deionized water before covering them with aluminum foil and then drying them in an oven at 40 °C. Water filtration was done under laminar flow and the glass equipment was covered with aluminum foil. All the bench tops were cleaned with ethanol and during all the laboratory procedures, cotton lab coats, clothing, and nitrile gloves were used. A control blank was utilized to assess the possible contamination levels by MPs during all the

laboratory analysis (filtration device, digestion with H_2O_2, and quantifications of MPs). Therefore, the MPs in the samples were counted after the subtraction of the MPs found in the blanks (2 to 3 items/blank).

2.7 Characterization of MPs in the SPM

Water samples were vacuum-filtered through a nitrocellulose filter (0.45 µm pore size, Millipore) using an aluminum foil-covered glass filtration. Filters were dried at room temperature, permanently covered to prevent contamination from airborne fibers and Petri dishes containing the filters were sealed until further analysis (Noren, 2007; Villagran et al. 2020). MPs were quantified and described based on their visual properties, such as shape, size, and color, using a stereomicroscope LEICA S8AP0 and an optical microscope Nikon Eclipse LV100 (Noren, 2007; Villagran et al. 2020). They were classified by size (<500 µm, 500–1,500 µm, 1,500–2,500 µm, 2,500–3,500 µm, 3,500–5000 µm, and >5000 µm). Fibers larger than 1,000 µm were manually separated using a hypodermic needle or dissection tweezers for further characterization techniques. Sub-samples of fibers were transferred to an Al mirror, and their chemical composition was determined using a Nicolet iN10 FT-IR Microscope. The obtained data was compared with the reference spectra of pure polymers. All the spectra were recorded in the range of 500 to 3,500 cm^{-1} with a resolution of 4 cm^{-1}. Analogously, for the surface characterization and elemental composition analyses by SEM/EDX, other sub-samples of fibers were placed over the copper tape on an SEM holder and analyzed using the same procedure and equipment detailed in section **2.5**.

3. Results and discussion

3.1 Environmental parameters

It has been demonstrated that the interaction between toxic pollutants and particulate matter depends mainly upon the physicochemical variables of the water column, as well the nature of the particles and the pollutants involved (Eisma, 1981; Souza Machado et al., 2015). In this study, temperature during the winter period in CP ranged between 7.4 °C and 11.2 °C, with a mean temperature of 9,0 °C (S.E: ±1.8), while pH on the surface water ranged from 7.12 to 8.81, with a mean value of 8.23 (S.E: ±0.75). The results indicated a mean value of salinity, and Chl-*a* of 31.75 PSU (S.E: ±3.84) and 2.67 µg.L^{-1} (S.E: ±1.70), respectively. The DO concentrations ranged from 6.42 to 9.31 mg.L^{-1} (mean: 8.62, S.E: ±2.12). These findings could be related to the low temperatures during that period, which favor oxygen solubility and also the photosynthesis process by the phytoplankton bloom (mainly of centric diatoms *Thalassiosira minima*) (Guinder et al., 2009; Fernández-Severini et al., 2012; Spetter et al., 2015a). However, Chl-*a* values were lower in comparison with those presented by Guinder et al. (2015), where the authors recorded levels of up to 25 µg.L^{-1} for the same winter-early spring season. These lower rangers recorded in our study might be due to grazing predation by micro and macro zooplanktonic species such as copepodites of *Eurytemora americana* that feed on small diatoms under low temperatures and high salinity, whereas adults of the same species feed on larger diatoms(Berasategui et al., 2009; 2012).

The SPM content and turbidity presented mean values of 16.06 mg.L^{-1} (S.E: ±2.86) and 14.0 NTU (S.E: ±4.76), respectively. Particularly, the levels of SPM were lower than those usually recorded in the study area (**Table 1).** This could be explained by a dry winter season of accumulated precipitations of 220.1 mm. The highest precipitation was registered in May (48.2 mm), while July did not register any, being this last one the driest month of the sampling. In the BBE, this implies that the winter

season corresponds to an atypical dry season for the SW Atlantic, that affects the biogeochemical cycles, the phytoplankton-nutrients relationship, the phenology and structure of plankton communities, the SPM, and the behavior of metals as it has been stated by other authors (Popovich and Marcovecchio, 2008; Guinder et al., 2010; Spetter et al., 2015a; Villagran, 2019b).

3.2. SPM characterization and interaction with heavy metals

The characterization of the SPM from the inner zone of the estuary (CP) by XRD and SEM/EDX, showed that it is enriched by diatoms frustules, radiolarians, other unidentified planktonic remains, detritus, and crystal materials (minerals) **(Figure 2** and **3).** During the sampling period, the mineralogical composition and the grain-size distribution profiles remained constant. The mineralogical composition of the SPM was represented mostly by quartz, feldspar, calcite, and, to a lesser extent, clay (**Figure 2a)**. In this sense, the clay fraction analysis indicated the presence of smectites as the main component followed by illite, interstratified minerals, chlorite, and kaolinite, in coincidence with a study by Grecco et al. (2006). The grain-size distribution profiles showed a predominant composition of fine to medium silt sediment. Most of the measurements were characterized by one mode, approximately between 30 and 70 μm, corresponding to silt very-fine sand particles with low clay content (**Figure 2b**). However, particles of ≤ 10 μm were also observed in the SEM images (**Figure 2c**). The EDX analysis (**Figure 2c**) revealed the presence of diatoms, diatomic remains (spectra 8 and 10) and minerals, such as feldspar and iron oxide (spectrum 9), supporting the mineralogical composition determined with XRD, although Fe and its species were expected to be the main components of SPM, they were only detected by EDX, XPS,

and ICP-OES. **Figure 3** shows the biological composition of the SPM, characterized by the presence of different phytoplankton species, most of them centric and pennate diatoms commonly found in the BBE. These results are in accordance with a study carried out by Guinder et al., (2009) during the phytoplanktonic winter bloom in the inner area of the BBE.

XPS is usually employed to identify the specific electron binding energies (B.E.) of the surface particles in marine sediments or soils (Gerin et al., 2003; Arnarson and Keil, 2007; Kim et al., 2014; Guan et al., 2017). **Figures 4a** and **4b** show the survey spectra of the untreated samples and those treated with H_2O_2, respectively. The relative element concentration based on the atomic states of the particles in the SPM samples is presented in **Table 1**. The main elements detected in both types of samples were O, Si, and in lower proportion Ca, N, Cl, C, Fe, Al, K, and Na **(Table 1)**. However, the SPM sample treated with H_2O_2 presented significant changes in the atomic percentage of N, C, and Ca, and also showed the presence of P **(Table 1)**. Therefore, phosphorus could have been released when part of the organic matter was eliminated (e.g., bacteria, algae, debris, phytoplankton, and smaller zooplankton captured in the filter) as a result of the action of H_2O_2. This behavior means that phosphorus could initially be inside the organisms and be released after the H_2O_2 treatment, and thus would only be detected in the treated samples, as XPS is a surface particle technique **(Figures 4a, 4b)**.

A detailed XPS analysis of specific electron B.E. of the elements in the untreated and treated SPM samples is illustrated in **Figures 5** and **6,** respectively**.** In **Figure 5a** (untreated SPM sample), the Si 2p spectrum can be fitted into three peaks with the following energy assignments: 102.65 eV to aluminosilicate; 101.87 eV to organic-Si (C, N) or Si-OH and 103.14 eV to SiO_2 (Tesson et al., 2009; Ma et al.,

2019). The presence of organic-Si can be associated with a large number of diatoms in the phytoplankton bloom during the sampling period. As for the treated sample, the Si 2p spectrum (**Figure 6a**) can also be fitted into three peaks with similar assignments as the Si spectrum of the untreated sample. However, the fitted peak at about 99.89 eV is associated with elemental Si (Tesson et al., 2009; Ma et al., 2019; Thermo Fisher Scientific Inc.). The spectrum of O 1s of the untreated SPM sample is shown in **Figure 5b.** The O 1s spectrum of the untreated sample contains contributions from metal-carbonates, metal-oxides, and oxygenated functional groups on the organic matter. The fitted peak of O 1s at about 531.40 eV corresponds to -OH, C-O-C, and C=O; the peaks at 530.50 eV and 531.80 eV are associated with metal oxides and metal carbonates, respectively (Flogeac et al., 2005; Shchukarev et al., 2008; Guan et al., 2017; Ma et al., 2019; Thermo Fisher Scientific Inc.). It should be noted that the metal oxides (Al_2O_3, Fe_2O_3) present their binding energy in the range of 528-531 eV (Seleţchi and Duliu, 2007; Shchukarev et al., 2008; Guan et al., 2017), while organic-Si and SiO_2 do it at 101 and 103 eV, respectively. Particularly, clay particles can adsorb metal ions via two different mechanisms that depend on pH: i) Cation exchange in the interlayers resulting from the interactions between ions and permanent negative charge and ii) Formation of inner-sphere complexes through surface hydroxyl groups (Si–O− and Al–O−) of the mineral surfaces. These groups could provide adsorption sites for dissolved metal cations and complex ions in seawater (Tamura et al., 2001; Abollino et al., 2003; Guan et al., 2017).

It can be observed that H_2O_2 treatment shifted the O 1s peak towards lower B.E. by ~0.5 eV compared to the untreated sample. Consequently, for the treated sample (**Figure 6b**), there is a significant shift in the position of the maximum peak in O 1s. The B.E. positions are observed at 531.58 and 530.50 eV associated with the metal-

carbonates and metal-oxides, whereas the peak corresponding to organic C=O was not detected (Omran et al., 2015; Guan et al., 2017). The spectrum of C 1s is presented in **Figure 5c**. The C 1s peak was deconvoluted into three peak components, at 284.75 and 288.83 eV, associated with the C-C and metal carbonate, and the third one located at 286.89 eV, corresponding to C-(O, N) (Flogeac et al., 2005; Seleţchi and Duliu, 2007; Ma et al., 2019).

The N 1s peak centered at 399.78 eV is displayed in **Figure 5d** and was also deconvoluted into one peak component at 399.80 eV associated with the amide or amine functions (Seleţchi and Duliu, 2007; Tesson et al., 2009; Ma et al., 2019). The position of the signal of C (284-286.4 eV) and N (402-398 eV) could be assigned to organic matter present in the sample (Flogeac et al., 2005; Seleţchi and Duliu, 2007). It is important to note that organic matter tends to form water-soluble/insoluble complexes with metal ions and hydrous oxides by interacting with mineral particles. Moreover, the relation obtained of Si, Al, and Fe by XPS at the surface of the SPM particles could indicate that the organic matter has affinity for adsorption on the mineral surfaces as alumino-silicate and quartz. In some alumino-silicates (clays), the general arrangement of Al and Si atoms is in layers, along with O atoms and -OH groups. Moreover, other cations, such as Fe, Mg, and K, may be included (Pilson and Island, 2013; Gorny et al., 2016).

The peaks of C 1s (B.E.~285 eV) and N 1s (B.E.~400 eV) in the treated samples are not shown because their signal were extremely weak and noisy. The P 2p peak was deconvoluted into one component at 133.55 eV associated with metal-phosphate (**Figure 6c**) (Tesson et al., 2009; Thermo Fisher Scientific Inc.). It is known that the PO_4^{3-} ion tends to be adsorbed on iron oxides and aluminium surfaces, and to

precipitate in the presence of divalent metals (Ca^{2+}, Mg^{2+}) or ferric ions (Fe^{3+}) (Bally et al., 2004; Spetter et al., 2015b).

Fe 2p spectra

For the untreated samples (**Figure 7a**), the Fe 2p spectrum contains two peaks of Fe $2p_{3/2}$ and Fe $2p_{1/2}$ at B.E. positions of ~711.79-711.38 and ~727.42–724.50 eV, respectively (Shchukarev et al., 2008; Guan et al., 2017). The Fe $2p_{3/2}$ peak was deconvoluted into three peak components; the peak at 709.14 eV associated with FeO (Fe^{2+}), and the peaks at 711.39 and 713.03 eV, which correspond to iron oxides (Fe^{3+}) (Omran et al., 2015; Guan et al., 2017). In particular, it is known that the absence of the satellite peak between 718.28 and 718.48 eV can indicate the presence of Fe_3O_4 (and which can also be expressed as FeO. Fe_2O_3) (Mills and Sullivan, 1983; Taylor et al. 2006; Omran et al., 2015). The Fe $3p$ peak for Fe_3O_4 is not shown because the signal was extremely weak. Nevertheless, this result indicates that the Fe found is a mixture of Fe^{2+} and Fe^{3+} oxidation states, which contributes to the Fe $2p_{3/2}$ signal. It should be noted that the adsorption of iron oxy-hydroxides onto clay minerals is well documented and depends on the pH of the water (Boyle, 1977). The presence of Fe^{2+} on a mineral surface is commonly attributed to the complexation of Fe^{2+} by hydroxy ligands, which stabilize the Fe^{3+} oxidation state present in minerals (Gorny et al., 2016, Guan et al., 2017). Likewise, the mineral phases containing Fe^{2+} can contribute to the reduction of other redox-sensitive trace elements, such as chromium (Cr^{6+}) and arsenic (As^{5+}), among others (Gorny et al., 2016). For the treated samples (**Figure 7b**), the Fe 2p spectrum contains two peaks of Fe $2p_{3/2}$ and Fe $2p_{1/2}$. There is a significant shift in the position of the maximum peak in the Fe 2p doublet. The B.E. positions are observed for Fe $2p_{3/2}$ (~711.87–711.48 eV) and Fe $2p_{1/2}$ (~725.28–725.05 eV). The $2p_{3/2}$ peak

shifted into two components at 711.60 and 715.97 eV corresponding to iron oxides (Fe^{3+}) (Omran et al., 2015; Guan et al., 2017). These results indicate that after being treated with H_2O_2, the Fe^{2+} present in the sample (Fe^{2+}-organic matter) was oxidized to Fe^{3+}. According to the results obtained by XPS, it can be concluded that the speciation of iron in the SPM samples of the water column of CP is mostly iron Fe^{3+}, and Fe^{2+} in a lower proportion. These species are present as oxides or oxy-hydroxides on the surface of the mineral.

The mean concentration of heavy metals in the SPM during the sampling period is shown in **Table 2**. With the exception of Cu and Zn, the values of heavy metals in the SPM were lower than those usually recorded in this study area (**Table 2)** (Fernández Severini et al., 2017; 2018; Forero et al., 2020 submitted). Most of the particulate metal levels (Cr, Cu, Ni, Fe, and Mn) documented in this study may be due to the incorporation of these metal ions from the dissolved phase by phytoplankton bloom, that exhibited high abundance during the sampling period. In this sense, during phytoplankton bloom and compared with metal levels reported in periods before and after it, metals in the SPM significantly increased with the concomitant decline of their levels in the dissolved phase (Cabrita et al., 2020). Therefore, phytoplankton is likely to be a dominant sink of metals during the bloom period of winter. Ni, Fe, and Mn are essential elements for phytoplankton since they participate in photosynthesis. Twining and Baines (2013) highlighted that metal concentrations in phytoplankton are strongly associated to the biochemical demand of the cells, as well as environmental availability. The metal requirements of phytoplankton are functions of shifting light, macronutrient, and temperature regimes. Fe is considered the most abundant metal in phytoplankton and necessary in many biochemical processes like C and N fixation, nitrate and nitrite reduction, chlorophyll synthesis, as well as for the electron transport chain of

photosynthesis and respiration. In the case of Ni, it is associated primarily with urease and a Ni form of superoxide dismutase. Mn is involved in the O_2-evolving complex of photosystem II in the oxidation of water. It is also a common Mn form of superoxide dismutase in diatoms, and participates in phosphorylation reactions (Twining and Baines, 2013). Cr is not an essential element for phytoplankton and might have toxic effects for this community, whereas the most stable and common forms in estuarine environments are Cr^{3+} and Cr^{6+} (Souza Machado et al., 2015). The Cr^{6+} is the most toxic form, being efficiently uptaken by the cells through cellular channels, where this species suffers chemical reduction reactions that produce intermediate reactive species that are harmful to cell organelles, proteins, and nucleic acids (Dwivedi et al., 2010). Moreover, the mean concentration of toxic metals such as Cd (< MDL) and Pb (mean: 2.50 $\mu g.g^{-1}$ d.w, S.E:±0.84), were lower than the reported by Villagran et al., (2019a) and Fernández Severini et al., (2017) for the same site (**Table 2**). Although it is well known that Cd and Pb are some of the most common toxic pollutants that can be found in the water column of coastal environments with high anthropogenic pressures, such as the BBE, our values can be related to the anomalous low quantity of the SPM. In this sense, metal ions are mostly adsorbed on suspended particles. Thus, the low amount of the SPM recorded during the sampling period has a direct effect on the concentration of heavy metals in the water column (Andrade, 2001; Fernández Severini et al., 2017; Fernández Severini et al., 2009). Besides, physicochemical variables, such as pH, DO, and salinity can also affect the interaction between heavy metal ions and the SPM.

Particularly, the concentrations of Cd and Pb in CP are mostly associated with the particles of the SPM that come mainly from riverine runoffs (Fernández Severini et al., 2018). Cd is also associated with organophosphate compounds used in agricultural activities in the area (Buzzi and Marcovecchio, 2018) since it is present as an impurity

in the phosphate rocks. As a persistent pollutant, Pb might be in the estuary due to its use in gasoline in past decades as antiknock additive, and the petrochemical activities which are carried out in the estuary since the '80s. Some studies detected this metal in industrial soils (Albornoz et al., 2016) and agro ecosystems (Chen et al., 1997), suggesting that the sources of these metals in CP might be from regular industrial activities and diffuse sources such as pesticides with residues of Pb that enter the estuary from runoffs and drift. Although industrial and urban discharges are punctual sources, the extensive internal circulation mixing the estuary water and its high residence time result in the distribution of several pollutants, like these metals, throughout the internal zone of the estuary. (Perillo et al., 2001)

3.3. MPs characterization in the SPM and their interaction with heavy metals

MPs were quantified by color and size in the SPM samples. Fibers were the most abundant type of MPs, and nearly all of them were blue and black, whereas the number of fragments was insignificant (**Figure 8**). The MPs abundance in the water column at CP ranged from 2 to 11.5 items.L^{-1}, with an average of 6.50 items.L^{-1} (S.E: 4.01) (**Figure 9a** and **9b**). The most common size of fibers ranged from 500 to 1,500 µm, representing almost 41.76 % of the whole range of the fibers, while the remaining 58% comprises the other fiber range sizes (**Figure 9c)**. It is important to point out that CP receives the input of the sewage discharges from a treatment plant and domestic waters that might contribute to the presence of the MPs in the water column. In this regard, Fernández Severini et al., (2019) and Villagran et al., (2020) reported that the possible sources of MPs present in the water column of the BBE might be the sewage discharge from Bahía Blanca city, which has poor treatment, as well as fishing activities, and maritime traffic. Moreover, the discharge from the river Sauce Chico (1.9

$m^3.s^{-1}$) along with small freshwater tributaries could be other sources of plastic debris in the inner zone of the BBE.

MPs in the aquatic environments show a tendency to adsorb pollutants such as heavy metals, polycyclic aromatic hydrocarbons, organochlorine pesticides, and other persistent organic compounds (Wang et al., 2017; Guo and Wang, 2019; Yu et al., 2019). In our study, the interaction between metals and MPs can be inferred through SEM micrographs and EDX analysis applied to fibers present in the SPM. In this sense, **Figures 10a** and **b** show SEM micrograph and EDX analysis of the fibers present in the SPM. In particular, SEM image (**Figure 10a**) shows that the fiber is partially covered with other particles, which makes its observation and identification difficult. The mapped sample has a high concentration of carbon atoms characterized by the red zone shown in **Figure10(a1)**. EDX analysis of the fiber exhibited a strong C peak and small peaks of O, Fe, Ca, K, Na, Cl, and Si (**Figure 10a2**). **Figure 10b** shows a SEM image of a fiber section, in which a subsequent 4,000x magnification leads us to identify the deposition of small particles (probably clay minerals) on the smooth surface of the fiber. EDX analysis on two different surface sites of the fiber is also presented. Both sites exhibit elemental signals, but an additional sulfur peak is well denoted in site 2 (**Figure 10b1**). Also, some studies have reported fibers identified as MPs in surface sediments or air, based on a strong carbon signal obtained from EDX analysis (Fries et al., 2013; Blair et al., 2019). These authors reported that the presence of trace amounts of Al, Ca, Mg, Ti, Na, and Si indicate additive substances in plastic polymers or adsorbed debris on the MPs surface. SEM/EDX images also revealed that the MPs exhibited various mechanical erosion levels, such as cracks, flakes, and pits, and several small particles attached to the MPs surface (**Figure 11**). It is well known that the changes in surface roughness of plastics are due to material degradation with time (under permanent

exposition to external UV radiation, mechanical abrasion, temperature, among others.) (Wang et al., 2017; Yu et al., 2019). The rough surface increases the surface area of MPs, and it can carry hydrophobic/hydrophilic organic pollutants and heavy metals. From EDX spectra, elemental composition differences can be appreciated for three sites on the MPs surface (**Figure 11a** and **b**), indicating possible metals that are adsorbed or transported by MPs (Wang et al., 2017).

Once completed the optical analysis, about 20% of fibers samples were analyzed by FT-IR for their respective identification. **Figure 12** shows the spectra of analyzed fibers within a standard spectrum of cellulose-based textile fiber and poly(amide), respectively. As can be seen from Figure **12a** a good agreement is clearly visible both in peak position and intensity between MPs and reference material. In all cases, a broad band of about 3,400 cm^{-1} indicates the O-H stretching of the alcohol groups present in the polymer structure. In comparison, a set of signals at about 1,300 to 1,400 cm^{-1} and 1,000 to 1,100 cm^{-1} are originated by the C-OH bending and the C-O (or C-OH) stretching vibrations, respectively (Pretsch et al., 2009). The lack of intense and well-defined peaks in the region between 1,650 and 1,750 cm^{-1} indicates the absence of carbonyl or nitro groups, the reason why acetate or nitro cellulose-based materials were not considered as a constituent of those MPs. Thus, we suggest that the chemical composition of fibers analyzed is regenerated cellulose. In this sense, it is known that this kind of material gained much attention in the last decades as an inexpensive replacement of cotton in the textile and clothing industry, being Rayon, Viscose, Lyocell, or Modal, some examples of those commercial fibers. Although those materials began from natural and renewable sources such as soft-wood, its manufacturing implies several chemical treatments and the incorporation of additives, which convert them into anthropogenic pollutants. Finally, a considerable amount of these types of fibers

originated from the mechanical degradation of clothing textiles and hygiene products enter the aquatic environment through sewage, avoiding water treatment processes due to their flotation capacity (Browne et al., 2011). Therefore, and according to the previously discussed, the BBE, especially CP, is profoundly affected by domestic and industrial sewage discharges, which seem to be the major MPs constituent.

Our results coincide with a report by Wang et al., (2017), who evaluated the abundance, composition, surface texture, and interaction of MPs with heavy metals in the surface sediments from the littoral zone of the Baijiang River. These authors suggested that cellulose-based fibers are also prevalent in the environment, and they should be monitored since they can contain industrial dyes or additives, which are potentially dangerous for animals and humans due to their carcinogenic and toxicological effects. Dyachenko et al., (2017) also found cellulose-based fibers in wastewater treatment plants, while a framework reviewed by Dris et al., (2017) also supports the idea that cellulose-based MPs are due to domestic discharges, strengthening the idea that in CP, these MPs come from the same domestic source.

The spectrum originated by poly(amide) reference and microfiber sample are presented in **Figure 12b,** it can be seen the spectrum of the sample presents good similarity with respect to the reference. Signals at 3,070 and 3,300 cm^{-1} are assigned to the N-H stretching, while characteristic amide I and amide II bands are observed at 1,640 and 1,560 cm^{-1} (Pretsch et al., 2009). Poly(amide) is a material mainly used for the fabrication of fishing nets, ropes and strands intensively used in nautical activities, being Nylon 6 or Nylon 6.6, the most popular and inexpensive polymers used (Li et al., 2016). As it was previously mentioned, the influence of industrial activities and artisanal and recreational fisheries in the BBE are remarkable, along with the presence

of the most extensive port and Naval Base of the Argentine Navy (Base Naval Puerto Belgrano, Punta Alta), and thus, it could be expected to find small fragments of nets, ropes, and strands as part of the SPM.

In the recent two years, many papers have reported the interaction between MPs and metal ions (Pb, Zn, Ni, Cu) such as Tang et al. (2020;2021). In particular, Tang et al. (2020) studied under laboratory conditions, the adsorption process of Pb^{2+} ions on aged surface Nylon MPs as a function of fulvic acid concentration, ionic strength, and pH (Tang et al. 2020). These authors concluded that the adsorption of Pb^{2+} ions on Nylon MPs was spontaneous and endothermic, and this metal ion can form complexes with a surface carboxyl group on the surface of the MPs. Moreover, they also informed that the NaCl concentrations, initial solution pH, and fulvic acid have a significant effect on Pb^{2+} adsorption process on aged surface Nylon MPs. On the other hand, these same researchers also demonstrated that divalent metal ions as Ni^{2+}, Cu^{2+}, and Zn^{2+} could be interacting with some carboxylate anions through electrostatic attraction, as well as hydroxyl and carboxyl groups through chemisorption on surface Nylon MPs (Tang et al. 2021). According to environmental variables of the water column of BBE and the study reported by Tang et al. (2020;2021), the high values of salinity, alkaline pH, and dissolved organic matter of autochthonous origin (with low degree of aromaticity and microbial origin, Martinez personal communication) could be affecting the adsorption process of some heavy metal ions on aged Nylon microplastics present in the estuarine water. On the other hand, Fernandez Severini et al. (2020) found some black fragments and polymer fibers in the abdominal muscle of shrimps (*Pleoticus muelleri)* from the BBE. These polymeric particles exhibited some pollutants adsorbed (Br and Zn) on their surface, and inorganic plastic additives (barium salts) in their composition.

Though in our study, a battery of several metals and their possible association with MPs have been studied as well as their potentially toxic effects on the biota, further studies should include the effects of the interaction MPs-Hg and MPs-As. In the case of Hg-MPs, studies by Barboza et al. (2018a, b) evaluated the combined and single effect of Hg and MPs in the European seabass *Dicentrarchus labrax*. These authors concluded that MPs influence the bioaccumulation of Hg in the juveniles of this species. The mixture caused neurotoxicity (through acetylcholinesterase inhibition), oxidative stress (by increased lipid oxidation), and changes in the activity of energy-related enzymes (through changes in some dehydrogenases). Also, the combined effects of this metal and MPs reduced the swimming performance, its velocity and resistance time in *D. labrax*, and this could imply further effects on the population fitness (Barboza et al., 2018b). In the case of As-MPs, few studies analyzed this interaction and the possible ecotoxicological effects in marine organisms. Recently Dong et al. (2020) determined that As^{3+} was adsorbed on the surface of polystyrene microplastic particles (PSMPs) through hydrogen bonding with the carboxyl group. Thus PSMP could act as an Arsenic carrier with harmful effects on the biota. However, more research should be conducted in relation to the interaction between these toxic elements and MPs and their potential effects on organisms.

As a final remark, SPM and MPs are vectors of several pollutants, which can be potentially dangerous for aquatic organisms. The negative impacts are due to a cumulative effect of these vectors or to a potential synergic effect of vectors and pollutants. The harmful effects can be tracked in the interactions of metals with the fine fractions (silt-clay) of the SPM and sediments due to the high surface area that provide a proper site for the accumulation of heavy metals and other toxic substances (Souza Machado et al., 2015). Moreover, high concentrations of suspended solids in the water

column can generate adverse impacts on marine and coastal biodiversity. The MPs also provide a proper area with fractures, pits, roughness, besides their high hydrophobicity, among other factors that could enhance their toxic effect due to the accumulation of trace elements. The functional groups at polymer particle surfaces determine the surface charge properties that allow them to interact with ions or complexes. In this sense, some studies have found that the interaction between MPs and metals in the marine environment is associated with modification of MPs surface because of organic matter adhesion (Turner and Holmes, 2015;Wang et al., 2017). According to our results, the individual MPs fibers analyzed seem to carry the common metals present in the natural suspended particles, and these metals are relatively non-toxic. Finally, it is noteworthy that the association of MPs with heavy metals is strongly influenced by the presence and concentration of organic matter in the SPM and by the interaction with silt and clay minerals that accumulate metals.

4. Conclusion

We here report for the first time the chemical, geological, and biological composition of the SPM present in Cuatreros Port (BBE, Argentina) with different optical and spectroscopic tools. We also assessed the presence of MPs in the water column of this human-impacted estuary, the XPS, XRD, and SEM/EDX analyses revealed that the SPM is composed of MPs, diatoms frustules, other unidentified remains of plankton, detritus, and minerals such as quartz, feldspar, calcite, and clay (illite), with a particle size ranging between 30 to 70 μm. The XPS analyses showed the presence of metal-phosphate and Fe species (Fe^{2+} and Fe^{3+}) in the SPM. It was also feasible to detect the presence of heavy metals with ICP-OES, especially Cr, Ni, Fe, and Mn, and some of these metals, such as Fe, were also identified with SEM/EDX on MPs surfaces. Those results also established that the SPM acts as vectors of transport of

heavy metals in CP.

MPs encountered in the SPM were mostly fibers, of blue and black colors. The spectroscopic analyses showed that cellulose-based textile fibers and poly(amide) fibers were predominant. Moreover, mesoplastics (> 5 mm) were also found in the SPM. Therefore, the primary inputs of MPs in CP are likely to be untreated sewage discharges, small-scale artisanal fisheries, nautical activities, mostly present in the area, and riverine runoffs.

EDX spectra exhibited different types of elements in various sites on the fiber surface, such as Ti, Fe, and Al, suggesting that MPs are possible metal vectors in CP. Whereas the SEM images showed the presence of flakes, fractures, and small particles of minerals on the surface, demonstrating a weathering process in MPs that could also enhance their role as crucial vectors of trace elements.

Acknowledgements:

This study was part of a postdoctoral scholarship granted to Dr. A.D. Forero López by the National Scientific and Technical Research Council (CONICET), and part of it was funded with a PGI project granted to Dr. C. V. Spetter by the Universidad Nacional del Sur (PGI 24/Q109, UNS), both of Argentina. We also wish to thank Prof. Madeleine Raño for correcting the manuscript English language. To Lic. Benjamin Abasto, and Lic. Javier Arlenghi for their assistance in the field and all the staff of the Argentine Institute of Oceanography (IADO, CONICET-UNS).

Figure Captions

Figure 1. Map of the study area in the Bahía Blanca estuary. The point indicates the study site, Cuatreros Port (CP).

Figure 2. X-ray diffraction analysis **(a),** the grain size distribution profile **(b),** and SEM/ EXD micrograph for different particles present in the suspended particulate matter (SPM) at 3000x **(c)**.

Figure 3. SEM micrograph of the biological composition of the suspended particulate matter (SPM) obtained at different magnifications: **(a)** 1250x, **(b)** 2000x, **(c)** 2150x, **(d)** 4600x, **(e)** 6000x and **(f)** 8000x.

Figure 4. XPS survey spectrum of the suspended particulate matter (SPM) sample: **(a)** untreated and **(b)** treated with hydrogen peroxide (H_2O_2)

Figure 5. XPS survey spectrum of the untreated suspended particulate matter (SPM) samples. XPS intensities of: **(a)** Si 2p, **(b)** O 1s, **(c)** C 1s and **(d)** N 1s.

Figure 6. XPS survey spectrum of the treated suspended particulate matter (SPM) samples. XPS intensities of: **(a)** Si 2p, **(b)** O 1s and **(c)** P 2p.

Figure 7. Detail XPS spectra of Fe 2p and fitted Fe $2p_{3/2}$ spectra of the sample: **(a)** untreated and **(b)** treated with hydrogen peroxide (H_2O_2)

Figure 8. Images of microplastics (MPs) found in the samples of the suspended particulate matter (SPM).

Figure 9. Size range of the fibers according to the colors of the fibers **(a),** the percentage of colors **(b),** and the percentage of size range **(c)**.

Figure 10: (a). SEM micrograph, **(a1)** mapping image and **(a2)** EDX spectra of the fiber present in the suspended particulate matter (SPM); **(b)**. SEM micrograph and **(b1)** EDX spectra of the fiber present in the suspended particulate matter (SPM). SEM micrograph of the fiber at 4000x (Small insert).

Figure 11. SEM micrographs of MPs with magnification: **(a)** 3000x and **(b)** 7500x. Small insert: EDX spectra for three sites on the surface of the microplastics (MPs).

Figure 12. FT-IR spectra of microplastics (MPs) detected in the samples of the suspended particulate matter (SPM): **(a)** Cellulose-based textile and **(b)** Poly(amide).

References

Abollino, O., Aceto, M., Malandrino, M., Sarzanini C., Mentasti, E., 2003. Adsorption of heavy metals on vermiculite: Influence of pH and organic ligands. Water Res., 37 (7), 1619-1627. doi: 10.1016/S0043-1354(02)00524-9

Anbumani, S., Kakkar, P., 2018. Ecotoxicological effects of microplastics on biota: a review. Environ. Sci. Pollut. R., 25(15), 14373–14396. doi: 10.1007/s11356-018-1999-x

Andrade, S., 2001. Metales pesados en el agua de la zona interna de Bahía Blanca, y su toxicidad sobre algunas especies fitoplanctónicas. Doctoral Thesis, Universidad Nacional del Sur, p. 244.

Albornoz, C.B., Larsen, K., Landa, R., Quiroga, M.A., Najle, R., Marcovecchio, J.E., 2016. Lead and zinc determinations in Festuca arundinacea and Cynodon dactylon collected from contaminated soils in Tandil (Buenos Aires Province, Argentina). Environ. Earth Sci. 75(9), 181-190. doi:10.1007/s12665-016-5513-9

A.P.H.A. 1998. Standard methods for examinations of water and wastewater. Washington DC, 1193 pp.

Arias, A.H., Fernández Severini, M.D., Delucchi, F., Freije, R.H., Marcovecchio, J.E., 2010. Persistent pollutants monitoring in a South Atlantic coastal environment. Case

Study: The Bahía Blanca Estuary. In: Ortiz, A.C., Griffin, N.B., (Eds.). Pollution Monitoring. Nova Science Publishers, New York, USA, pp. 1-30.

Arnarson, T.S., Keil, R.G., 2007. Changes in organic matter–mineral interactions for marine sediments with varying oxygen exposure times. Geochim. Cosmochim. Acta 71(14), 3545–3556. doi:10.1016/j.gca.2007.04.027.

Atwood E.C., Falcieri F.M., Piehl S., et al 2019. Coastal accumulation of microplastic particles emitted from the Po River, Northern Italy: Comb[illegible]ing remote sensing and hydrodynamic modelling with in situ sample collections. Mar. Pollut. Bull. 138, 561–574. doi: 10.1016/j.marpolbul.2018.11.045

Bally G., Mesnage V., Deloffre J., Clarisse C., R. Lafite R., Dupont J.-P., 2005. Chemical characterization of pore waters in an intertidal mudflat of the Seine estuary: relationship to erosion–deposition cycles. Mar. Pollut. Bull., 49 (3), 163-173. doi: org/10.1016/j.marpolbul.2004.02.005.

Barboza, L. G. A., Vieira, L. R., Branco, V., Figueiredo, N., Carvalho, F., Carvalho, C., Guilhermino, L., 2018a. Microplastics cause neurotoxicity, oxidative damage and energy-related changes and interact with the bioaccumulation of mercury in the European seabass, *Dicentrarchus labrax* (Linnaeus, 1758). Aquat. Toxicol. 195, 49-57. doi:10.1016/j.aquatox.2017.12.008

Barboza, L. G. A., Vieira, L. R., Guilhermino, L., 2018b. Single and combined effects of microplastics and mercury on juveniles of the European seabass (*Dicentrarchus labrax*): Changes in behavioural responses and reduction of swimming velocity and resistance time. Environ. Pollut., 236, 1014–1019. doi:10.1016/j.envpol.2017.12.082

Berasategui, A.A., Hoffmeyer, M.S., Biancalana, F., Fernandez Severini, M.,

Menendez, M.C., 2009. Temporal variation in abundance and fecundity of the invading copepod Eurytemora americana in Bahía Blanca Estuary during an unusual year. Estuar. Coast. Shelf Sci. 85(1), 82–88. doi:10.1016/j.ecss.2009.03.008

Berasategui, A.A., Hoffmeyer, M.S., Dutto, M.S., Biancalana, F., 2012. Seasonal variation in the egg morphology of the copepod Eurytemora americana and its relationship with reproductive strategy in a temperate estuary in Argentina. ICES J. Mar. Sci. 69(3), 380–388. doi:10.1093/icesjms/fsr192

Blair, R.M., Waldron, S., Gauchotte-Lindsay, C., 2019. Average daily flow of microplastics through a tertiary wastewater treatment plant over a ten-month period. Water Res., 114909-114916. doi:10.1016/j.watres.2019.114909

Boyle, E.A., Sclater, F.R., Edmond, J.M. 1977. The distribution of dissolved copper in the Pacific. Earth Planet. Sci. Lelt., 34, 36-54.

Browne M.A., Crump P., Stewart J. N., Teuten E., Tonkin A., Galloway T., Thompson R., 2011. Accumulation of Microplastic on Shorelines Woldwide: Sources and Sinks. Environ. Sci. Technol. 45 (21), 9175-9179. doi: 10.1021/es201811s

Buzzi, N.S., Marcovecchio, J.E., 2018. Heavy metal concentrations in sediments and in mussels from Argentinean coastal environments, South America. Environ. Earth Sci., 77(8),321. doi:10.1007/s12665-018-7496-1

Cabrita, M.T., Brito P., Caçador I., Duarte B., 2020. Impacts of phytoplankton blooms on trace metal recycling and bioavailability during dredging events in the Sado estuary (Portugal). Mar. Pollut. Res. 153, 104837.

Chen, T.B.,. Wong, J.W.C, Zhou H.Y., Wong M.H., 1997. Assessment of trace metal

distribution and contamination in surface soils of Hong Kong. Environ. Pollut. 96(1), 61-8 doi: 10.1016/S0269-7491(97)00003-1

Cienfuegos, F., Vaitsman, D., 2000. Análise instrumental. Rio de Janeiro: Interciência, pp. 606 .

Cochran, J.K., 2014. Estuaries: where rivers meet the sea. Ref. Modul. Earth. Syst. Environ. Sci., 1–4. doi: 10.1016/B978-0-12-409548-9.09151-X

Critchell K., Hoogenboom, M.O. 2018. Effects of microplastic exposure on the body condition and behaviour of planktivorous reef fish (Acanthochromis polyacanthus). PLoS ONE 13(3),e0193308- e0193321. doi: 10.1371/journal.pone.0193308.

Cuadrado, D.G., Pizani, N., 2007. Identification of microbially induced sedimentary structures over a tidal flat. Lat. Am. J. Sed. Bas. Anal. 14(2), 105-116.

Dris, R., Gasperi, J., Mirande, C., Mandin, C., Guerrouache, M., Langlois, V., Tassin, B., 2017. A first overview of textile fibers, including microplastics, in indoor and outdoor environments. Environ. Pollut. 221, 453–458. doi:10.1016/j.envpol.2016.12.013

Dong, Y., Gao, M., Song, Z., Qiu, W., 2020. As(III) adsorption onto different-sized polystyrene microplastic particles and its mechanism. Chemosphere, 124792. doi:10.1016/j.chemosphere.2019.124792

Dwivedi, S., Srivastava, S., Mishra, S., Kumar, A., Tripathi, R.D., Rai, U.N., Dave, R., Tripathi, P., Charkrabarty, D., Trivedi, P.K., 2010. Characterization of native microalgal strains for their chromium bioaccumulation potential: Phytoplankton response in polluted habitats. J. Hazard. Mater. 173, 95–101. doi: 10.1016/j.jhazmat.2009.08.053.

Dyachenko, A., Mitchell, J., Arsem, N., 2017. Extraction and identification of microplastic particles from secondary wastewater treatment plant (WWTP) effluent. Anal. Methods 9(9), 1412–1418. doi:10.1039/c6ay02397e

Eisma, D., 1981. Chapter 9: Suspended matter as a carrier for pollutants in estuaries and the sea. Elsevier Oceanogr. Ser. 27, 281–295. doi: 10.1016/S0422-9894(08)71414-4.

EPA Environmental Protection Agency's (2016) Definition and Procedure for the Determination of the Method Detection Limit, 40 CFR 136 Appendix B; Revision 2, EPA Office of Water, EPA 821-R-16-006

Federal Register (1984) Definition and procedure for determination of the method detection limit. EPA, 40 CFR Part 136, Appendix B, Revision 1.11 1 (11), pp. 198–199.

Fernández Severini, M.D., Botté, S.E., Hoffmeyer, M.S., Marcovecchio, J.E., 2010. Lead concentrations in zooplankton, water, and particulate matter of a Southwestern Atlantic temperate estuary (Argentina). Arch. Environ. Contam. Toxicol., 61(2), 243–260. doi: 10.1007/s00244-010-9613-3

Fernández Severini, M.D., Hoffmeyer, M.S., Marcovecchio, J.E., 2012. Heavy metals concentrations in zooplankton and suspended particulate matter in a southwestern Atlantic temperate estuary (Argentina). Environ. Monitor. Assess. 185(2), 1495–1513. doi: 10.1007/s10661-012-3023-0

Fernández Severini M.D., Villagran D.M., Biancalana F., et al 2017. Heavy Metal Concentrations Found in Seston and Microplankton from an Impacted Temperate Shallow Estuary along the Southwestern Atlantic Ocean. J Coast Res 335, 1196–1209. doi: 10.2112/jcoastres-d-16-00151.1

Fernández Severini M.D., Carbone M.E., Villagran D.M., Marcovecchio J.E., 2018. Toxic metals in a highly urbanized industry-impacted estuary (Bahia Blanca Estuary, Argentina): spatio-temporal analysis based on GIS. Environ Earth Sci 77, 399-400. doi: 10.1007/s12665-018-7565-5

Fernández Severini, M.D., Villagran, D.M., Buzzi, N.S., Chatelain-Sartor, G., 2019. Microplastics in oysters (Crassostrea gigas) and water at the Bahía Blanca Estuary (Southwestern Atlantic): An emerging issue of global concern. Reg. Stud. Mar. Sci. 32, 100829-100840. doi: 10.1016/j.rsma.2019.100829.

Fernandez Severini, M.D., Buzzi N.S., Forero López A.D., Colombo C., Chatelain Sartor G.L., Rimondino G.N., Truchet D.M., 2020. Microplastics chemical characterization and abundance in the commercial shrimp *Pleoticus muelleri* at an impacted coastal environment (Southwestern Atlantic). Marine Pollution Bulletin (under review).

Flogeac K., Guillon E., Aplincourt M., Marceau E, Stievano L., et al., 2005. Characterization of soil particles by X-ray diffraction (XRD), X-ray photoelectron spectroscopy (XPS), electron paramagnetic resonance (EPR) and transmission electron microscopy (TEM). Agronomy for Sustainable Development, Springer, 25 (3), 345-353.

Forero López A.D., Villagran D.M., Fernández Severini M.D., Spetter C.V., Buzzi N.S. Chromium behavior and environmental impact in a highly urbanized estuary. The Bahía Blanca Estuary, SW Atlantic (Argentina) as a case study. Submitted Science of Total Environment. (under review).

Freije, R.H., Marcovecchio, J.E., 2004. Oceanografía Química. In: Piccolo M.C.,

Hoffmeyer, M.S. (Eds.) Ecosistema del Estuario de Bahía Blanca. Bahía Blanca, Argentina. pp. 69-78.

Freije, R.H., Spetter, C.V., Marcovecchio, J.E., Popovich, C.A., Botté, S.E., Negrín V.L., Arias, A.H., Delucchi F., Asteasuain, R.O., 2008. Water chemistry of Bahía Blanca Estuary. In: Neves, R., Baretta, J., Mateus, M. (Eds). Perspectives on Integrated Coastal Zone Management in South America, IST Press, pp. 241-254.

Frère, L., Maignien, L., Chalopin, M., et al., 2018. Microplastic bacterial communities in the Bay of Brest: Influence of polymer type and size. Environ. Pollut. 242, 614–625. doi: 10.1016/j.envpol.2018.07.023.

Fries, E., Dekiff, J.H., Willmeyer, J., Nuelle, M.T., Ebert, M., Remy, D., 2013. Identification of polymer types and additives in marine microplastic particles using pyrolysis-GC/MS and scanning electron microscopy. Environ. Sci. Proc. Imp. 15(10), 1949-1957. doi: 10.1039/c3em00214d.

Galvão, E.S., Santos, J.M., Lima, A.T., Reis, N.C., Orlando, M.T.D., Stuetz, R.M., 2018. Trends in analytical techniques applied to particulate matter characterization: A critical review of fundamentals and applications. Chemosphere, 199, 546–568. doi:10.1016/j.chemosphere.2018.02.034

Gelós, E.M., Marcos, A.O., Spagnuolo, J.O, Schillizzi, R.A., 2004. Textura y mineralogía de sedimentos de la Bahía Blanca. In: Piccolo M.C., Hoffmeyer, M.S. (Eds.) Ecosistema del Estuario de Bahía Blanca. Bahía Blanca, Argentina. pp. 43-50.

Gerin, P.A., Genet, M.J., Herbillon, AJ., Delvaux, B., 2003. Surface analysis of soil material by X- ray photoelectron spectroscopy. Eur. J. Soil Sci. 54(3), 589-604. doi: 10.1046/j.1365-2389.2003.00537.x

GESAMP., 2015. Sources, fate and effects of MP in the marine environment: A global assessment. J. Ser. GESAMP Reports Stud. pp. 90-98.

Gorny, J., Billon, G., Noiriel, C., Dumoulin, D., Lesven, L., Madé, B., 2016. Chromium behavior in aquatic environments: a review. Environ. Revi. 24(4), 503–516. doi:10.1139/er-2016-0012

Grecco, L.E., Marcos, A.O., Gómez, E.A., Botté, S., Marcovecchio, J., 2006. Natural and anthropogenic input of heavy metals in sediments from Bahía Blanca Estuary (Argentina). J. Coast. Res., 1021-1025.

Guan, C., Jiang, J., Pang, S., Luo, C., Ma, J., Zhou, Y., Yang, Y., 2017. Oxidation kinetics of bromophenols by nonradical activation of peroxydisulfate in the presence of carbon nanotube and formation of brominated polymeric products. Environ. Sci. Technol. 51(18), 10718-10728. doi: 10.1021/acs.est.7b02271. Epub

Guinder, V.A., Popovich, C.A., Perillo, G.M.E., 2009. Particulate suspended matter concentrations in the Bahía Blanca Estuary, Argentina: implication for the development of phytoplankton blooms. Estuar. Coast. Shelf. Sci. 85, 157–165. doi: 10.1016/j.ecss.2009.03.022

Guinder, V.A., Popovich, C.A., Molinero, J.C., Perillo, G.M.E., 2010. Long-term changes in phytoplankton phenology and community structure in the Bahı´a Blanca Estuary, Argentina. Mar. Biol. 157, 2703–2716. doi: 10.1007/s00227-010-1530-5

Guinder, V.A., Popovich, C.A., Perillo, G.M.E., 2011. Phytoplankton and physicochemical analysis on the water system of the temperate estuary in South America: Bahía Blanca Estuary, Argentina. Int. J. Environ. Res. 6 (2), 547-556. doi: 10.22059/IJER.2012.524

Guinder, V.A., López-Abbate, M.C., Berasategui, A.A., Negrin, V.L., Zapperi, G., Pratolongo, P.D., Fernández-Severini, M.D., Popovich, C.A., 2015. Influence of the winter phytoplankton bloom on the settled material in a temperate shallow estuary. Oceanologia, 57(1), 50–60. doi:10.1016/j.oceano.2014.10.002

Guo, X., Wang, J., 2019. The chemical behaviors of microplastics in marine environments: a review. Mar. Pollut. Bull. 142, 1–14. doi: 10.1016/j.marpolbul.2019.03.019

Harris L.S.T, Carrington E., Harbor F., 2019. Impacts of microplastic vs . natural abiotic particles on the clearance rate of a marine mussel. Limnol. Oceanogr. Lett. (ASLO), 1-8 doi: 10.1002/lol2.10120

Håkanson, L., 2006. The relationship between salinity, suspended particulate matter and water clarity in aquatic systems. Ecol. Res. 21, 75–90. doi: 10.1007/s11284-005-0098-x

Kim, E.J., Yoo, J.C., Baek, K., 2014. Arsenic speciation and bioaccessibility in arsenic-contaminated soils: Sequential extraction and mineralogical investigation. Environ. Pollut. 186, 29–35. doi:10.1016/j.envpol.2013.11.032

Lambert, S., Wagner, M., 2018. Microplastics are contaminants of emerging concern in freshwater environments: an overview. In Wagner, M., Lambert, S. (Eds.). Freshwater microplastics: emerging environmental contaminants? Springer Open, pp. 1-25.

Leslie, H.A., van der Meulen, M.D., Kleissen, F.M., Vethaak, A.D., 2011. Microplastic litter in the Dutch marine environment: Providing facts and analysis for Dutch policymakers concerned with marine microplastic litter. Deltares Report, p. 97.

Li, W.C., Tse H.F., Fok L., 2016. Plastic waste in the marine environment: A review of

sources, occurrence and effects. Sci. Total Environ. 566–567, 333-349. doi:.org/10.1016/j.scitotenv.2016.05.084.

Limbozzi, F., Leitao, T.E., 2008. Characterization of Bahía Blanca main existing pressures and their effects on the state indicators for surface and groundwater quality. Perspectives on integrated coastal zone management in South America. IST Press, Lisbon, pp. 315-331.

Ma, J., Zhou, B., Duan, D., Pan, K., 2019. Salinity-dependent nanostructures and composition of cell surface and its relation to Cd toxicity in an estuarine diatom. Chemosphere 215, 807-814. doi: 10.1016/j.chemosphere.2018.10.128

Marcovecchio, J.E., 2000. Land-based sources and activities affecting the marine environment at the Upper Southwestern Atlantic Ocean: an overview. UNEP Regional Seas Reports & Studies N°170: 67 pp.

Meybeck, M., Horowitz, A., Grosbois, C., 2004. The geochemistry of Seine River Basin particulate matter: distribution of an integrated metal pollution index. Sci. Total Environ. 328(1-3), 219–236. doi:10.1016/j.scitotenv.2004.01.024

Mills, P., Sullivan, J.L., 1983. A study of the core level electrons in iron and its three oxides by means of X-ray photoelectron spectroscopy. J. Phys. D: Appl. Phys. 16, 723

Noren, Frederick. Small plastic particles in coastal Swedish waters. *Kimo Sweden*, 2007, vol. 11.

Ogonowski, M., Motiei, A., Ininbergs, K., Hell, E., Gerdes, Z., Udekwu, K. I., Bacsik Z., Gorokhova, E., 2018. Evidence for selective bacterial community structuring on microplastics. Environ. Microbiol. 20(8), 2796-2808. doi:10.1111/1462-2920.14120

Omran, M., Fabritius, T., Elmahdy, A. M., Abdel-Khalek, N.A., Gornostayev, S., 2015. Improvement of phosphorus removal from iron ore using combined microwave pretreatment and ultrasonic treatment. Sep. Purif. Technol. 156, 724–737. doi:10.1016/j.seppur.2015.10.071

Perillo, G.M.E., Piccolo, M.C., Parodi, E., Freije, R.H., 2001. The Bahia Blanca estuary, Argentina. In: Seeliger, U., Kjerfve, B. (Eds.) Coastal marine ecosystems of Latin America. Springer, Heidelberg, pp 205–217.

Piccolo, M.C., Díez, P.G., 2004. Meteorología de Puerto Coronel Rosales. In: Piccolo, M.C., Hoffmeyer, M.S. (Eds.) Ecosistema del Estuario de Bahía Blanca. Bahía Blanca, Argentina, pp. 87-90.

Pilson M.E.Q., Island, R., 2013. An Introduction to the Chemistry of the Sea. Cambridge University Press, p. 524.

Popovich, C.A., Marcovecchio, J.E., 2008. Spatial and temporal variability of phytoplankton and environmental factors in a temperate estuary of South America (Atlantic coast, Argentina). Cont. Shelf Res., 28(2), 236–244.

Pretsch E., Bühlamnn P., Badertscher M., 2009. Structure and determination of organic compounds (4 Eds.) Enlarged Edition. pp. 17.

Seleţchi, E.D., Duliu, O.G., 2007. Comparative study on ESR spectra of carbonates. Rom. Journ. Phys. 52 (5-7), 657–666.

Shang, D., Xu, H., 2018. Qualitative dynamics of suspended particulate matter in the Changjiang estuary from geostationary ocean color images: An empirical, regional modeling approach. Sensors 18. doi: 10.3390/s18124186

Shchukarev, A., Gälman, V., Rydberg, J., Sjöberg, S., Renberg, I., 2008. Speciation of iron and sulphur in seasonal layers of varved lake sediment: an XPS study. Surf Interface Anal. 40 (3-4), 354–357. doi:10.1002/sia.2704

Silva, A.B., Bastos, A.S., Justino, C. I.L., da Costa, J. P., Duarte, A.C., Rocha-Santos, T.A.P., 2018. Microplastics in the environment: Challenges in analytical chemistry - A review. Anal. Chim. Acta. 1017, 1–19. doi: 10.1016/j.aca.2018.02.043

Spetter, C.V., Popovich, C.A., Arias, A., Asteasuain, R.O., Freije, R. H., Marcovecchio, J.E., 2015a. Role of nutrients in phytoplankton development during a winter diatom bloom in a eutrophic South American estuary (Bahía Blanca, Argentina). J. Coast. Res. 299, 76–87. doi:10.2112/jcoastres-d-12-00251.1

Spetter, C.V., Buzzi, N.S., Fernández, E.M.., Cuadrado, D.G, Marcovecchio, J.E., 2015b. Assessment of the physicochemical conditions sediments in a polluted tidal flat colonized by microbial mats in Bahía Blanca Estuary (Argentina). Mar. Pollut. Bull. 9, 491-505. doi: 10.1016/j.marpolbul.2014.10.008.

Souza Machado, A.A., Spencer, K., Kloas, W., Toffolon, M., Zarfl, C., 2015. Metal fate and effects in estuaries: A review and conceptual model for better understanding of toxicity. Sci. Tot. Environ. 541, 268–281. doi:10.1016/j.scitotenv.2015.09.045.

Sun, X., Liang, J., Zhu, M., Zhao, Y., Zhang, B., 2018. Microplastics in seawater and zooplankton from the Yellow Sea. Environ. Pollut. 242, 585–595. doi: 10.1016/j.envpol.2018.07.014

Tamura H., Mita K., Tanaka A., et al., 2001. Mechanism of hydroxylation of metal oxide surfaces. Journal of Colloid and Interface Science, 243(1): 202–207.

Tang, S., Lin, L., Wang, X., Feng, A., & Yu, A. 2019. Pb(II) uptake onto nylon microplastics: Interaction mechanism and adsorption performance. Journal of Hazardous Materials, 121960. doi:10.1016/j.jhazmat.2019.121960-

Tang, S., Lin, L., Wang, X., Yu, A., & Sun, X. 2020. Interfacial interactions between collected nylon microplastics and three divalent metal ions (Cu(II), Ni(II), Zn(II)) in aqueous solutions. Journal of Hazardous Materials, 123548. doi:10.1016/j.jhazmat.2020.123548

Taylor P., Frost D.C., Ishitani A., Mcdowell C.A., 2006. Molecular Physics : An International Journal at the Interface Between Chemistry and Physics X-ray photoelectron spectroscopy of copper compounds. 37–41.

Tesson, B., Genet, M.J., Fernandez, V., Degand. S., Rouxhet, P.G., Martin-Jézéquel, V., 2009. Surface chemical composition of diatoms. Chembiochem. 10 (12), 2011-2024. doi: 10.1002/cbic.200800811

Truchet, D.M., Noceti, M.F., Villagrán, D.M., Orazi. M.M., Medrano, M.C., Buzzi, N.S., 2019. Fishers' ecological knowledge about marine pollution: What can FEK contribute to ecological and conservation studies of a Southwestern Atlantic estuary. J. Ethnobiol. 39(4), 584-606. doi:10.2993/0278-0771-39.4.584

Turner, A., Millward, G.E., 2002. Suspended particles: Their role in estuarine biogeochemical cycles. Estuar. Coast. Shelf. Sci. 55, 857–883. doi: 10.1006/ecss.2002.1033.

Turner, A., Holmes, L.A., 2015. Adsorption of trace metals by microplastic pellets in fresh water. Environ Chem 12:600–610. doi: 10.1071/EN14143

Twining, B.S. and Baines, S.B., 2013. The Trace Metal Composition of Marine Phytoplankton. Annual Review of Marine Science 5: 191-215.

Vendel, A.L., Bessa, F., Alves, V.E.N, Amorin, A.L.A, Patrício, J., Palma A.R.T., 2017. Widespread microplastic ingestion by fish assemblages in tropical estuaries subjected to anthropogenic pressures. Mar. Pollut. Bull. 117:448–455. doi: 10.1016/j.marpolbul.2017.01.081

Villagran, D.M., Truchet, D.M., Buzzi, N.S., Forero López. A.D., Fernández Severini, M.D., 2020. A baseline study of microplastics in the burrowing crab (Neohelice granulata) from a temperate southwestern Atlantic estuary. Mar. Pollut. Bull. 150, 110686-110691. doi: 10.1016/j.marpolbul.2019.110686

Villagrán, D.M., 2019b. Dinámica de metales pesados en el material particulado en suspensión y plancton en ambientes costeros afectados por descargas de origen antrópico. Doctoral Thesis, Universidad Nacional del Sur, p. 151.

Von Moos, N., Burkhardt-Holm, P., Köhler, A., 2012. Uptake and effects of microplastics on cells and tissue of the blue mussel Mytilus edulis L. after an experimental exposure Environ. Sci. Technol., 46(20), 11327–11335. doi:10.1021/es302332w

Wang, W., Ndungu, A.W., Li, Z., Wang, J., 2017. Microplastics pollution in inland freshwaters of China: A case study in urban surface waters of Wuhan, China. Sci. Total Environ. 575, 1369–1374. doi:10.1016/j.scitotenv.2016.09.213

Wright, S.L., Thompson, R.C., Galloway, T.S., 2013. The physical impacts of microplastics marine. Environ. Pollut., 178, 483–492. doi: 10.1016/j.envpol.2013.02.031

XPs TS (2020) https://xpssimplified.com/periodictable.php. In: thermo Sci. XPs. https://xpssimplified.com/periodictable.php

Yu, F., Yang, C., Zhu, Z., Bai, X., Ma, J., 2019. Adsorption behavior of organic pollutants and metals on micro/nanoplastics in the aquatic environment. Sci. Total. Environ. 694, 133643-133654. doi: 10.1016/j.scitotenv.2019.133643

Zettler, E.R., Mincer, T.J., Amaral-Zettler, L.A., 2013. Life in the "plastisphere": Microbial communities on plastic marine debris. Environ. Sci. Technol. 47, 7137–7146. doi: 10.1021/es401288x

Credit Author Statement

Forero-López A. D.: Conceptualization, Methodology, Resources, Computations, Writing original draft preparation, Writing- Reviewing & Editing, Supervision.

Truchet D. M.: Visualization, Writing - Review & Editing.

Rimondino G. N.: Resources, Methodology, Writing - Review & Editing.

Buzzi N. S.: Methodology, Writing- Reviewing & Editing, Visualization.

Maisano L.: Resources, Methodology, Writing.

Spetter C.V.: Methodology, Writing- Reviewing & Editing.

Nazzarro M.S.: Resources, Methodology, Writing- Reviewing & Editing, Visualization.

Malanca F.E.: Resources, Methodology, Writing - Review & Editing.

Furlong O.: Methodology, Writing- Reviewing & Editing, Visualization.

Fernández-Severini M. D.: Methodology, Writing- Reviewing & Editing, Visualization, Supervision.

CONICET
U N S

August 10, 2020

Editor SCIENCE OF THE TOTAL ENVIROMENT

Conflict of interest:

The authors declare that they have no known competing financial interests or personal relationships that could have appeared to influence the work reported in this paper.

Sincerely yours,

Dra. Ana D. Forero-López

On behalf of all the co-authors

Table 1. Atomic percentage (determined by XPS) of the untreated suspended particulate matter (SPM) samples, and treated with hydrogen peroxide (H_2O_2)

Samples	Atomic percentage (%)										
	O	**C**	**Si**	**Al**	**Ca**	**Fe**	**Na**	**N**	**Cl**	**K**	**P**
Sample untreated	55.3	9.8	21.6	5.8	2.5	1.8	1.2	1.0	0.6	0.4	ND
Sample treated with H_2O_2.	54.85	7.22	22.0	5.7	3.9	1.67	1.61	0.54	0.9	0.6	1.3

Table 2. Mean concentrations (± SD) of heavy metals (µg g $^{-1}$ dw) in the suspended particulate matter (SPM). Comparison with mean heavy metals of the other studies reported in the Bahia Blanca Estuary (BBE).

Location	SPM (mg.L^{-1})	Cd	Cu	Cr	Fe	Mn	Ni	Pb	Zn	References
BBE, Argentina, CP	16.06 ± 2.86	< MDL	46.35 ± 5.02	3.15 ± 1.02	2,985 ± 1,634,83	12[illegible]5 ± [illegible].94	1.15 ± 0.37	2.5 ± 0.84	103.5 ± 37.48	This study
BBE, Argentina	46.13±17.04	0.07–0.63	21.87-49.06	4.99-23.98	15,67[illegible]-6[illegible]590	11.57–702.7	4.91–18.14	5.34–.14.1	50.6–93.42	Fernández Severini et al. (2017)
BBE, Argentina	----	< 0.03–16.26	-----	< 0.06–27.[illegible]	-----	-----	0.05–80.52	0.04–78.43	------	Fernández Severini et al. (2018)
BBE, Argentina, CP	71.96 ± 28.75	0.43 ± 0.22	17.08± 3.61	1[illegible].2 ± 2.24	25,470 ± 4613	548.5 ± 99	9.37± 1.92	5.41± 2.16	55.51 ± 14.6	Forero et al. (unpublished data)
BBE, Argentina, CP	80.96 ± 43.67	0.37 ± 0.30	19.4[illegible]± [illegible].03	15.22 ± 5.06	29,558 ± 8426	558.8 ± 148.2	11.13± 3.39	7.70± 5.22	60.98 ± 14.6	Villagrán et al. (2019b)

Graphical abstract

Highlights

- First detailed assessment of suspended particulate matter (SPM) and microplastics (MPs) in the Bahía Blanca Estuary.
- Metal-phosphates bonds and mixtures of Fe^{3+}/Fe^{2+} were detected in the SPM.
- Cr, Ni, Fe, Cd, Zn, Pb, and Mn were detected in the SPM
- MPs abundance ranged 3 to 11.5 items.L^{-1}
- MPs were mostly represented by semi-synthetic cellulose fibers and poly(amide)
- SPM and MPs as the main transport vectors for metals in the Bahía Blanca Estuary.

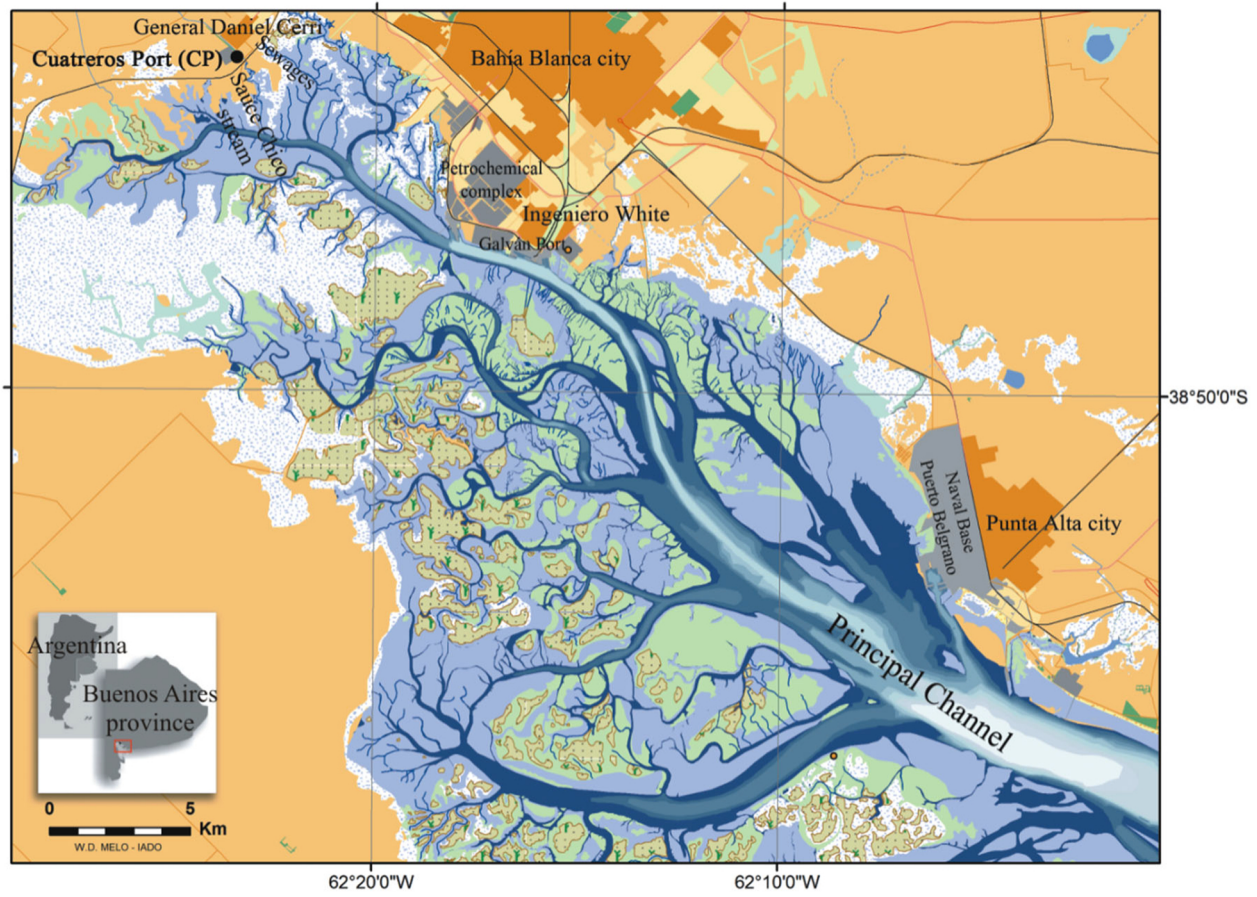
General Daniel Cerri
Cuatreros Port (CP)
Sewages
Sauce Chico
Stream
Bahía Blanca city
Petrochemical complex
Ingeniero White
Galván Port
38°50'0"S
Naval Base Puerto Belgrano
Punta Alta city
Principal Channel
Argentina
Buenos Aires province
0
5
Km
W.D. MELO - IADO
62°20'0"W
62°10'0"W

Figure 1

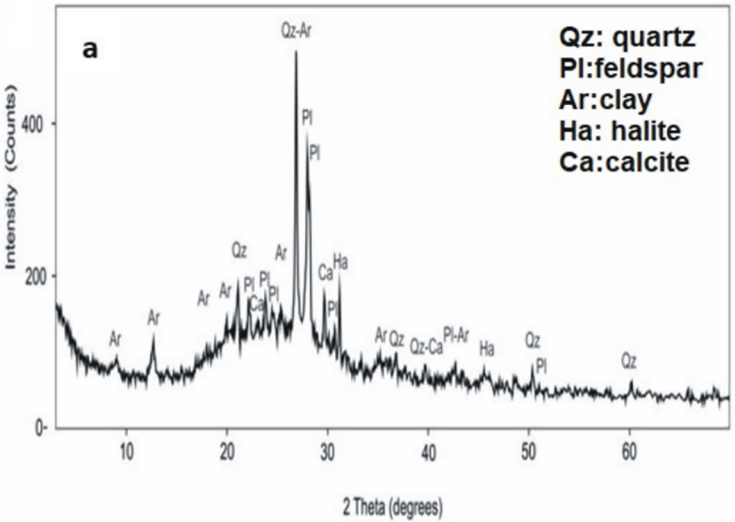

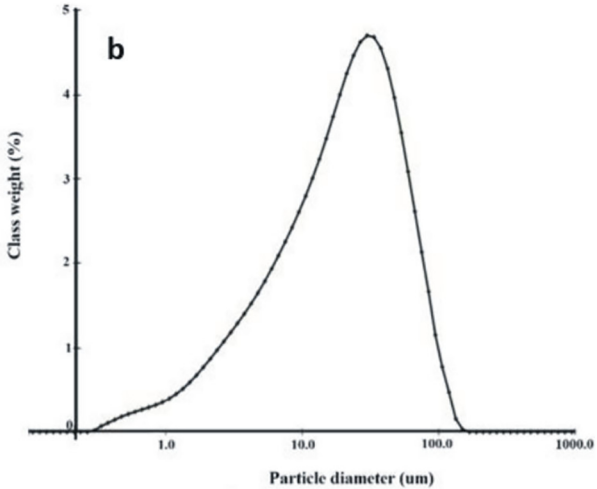

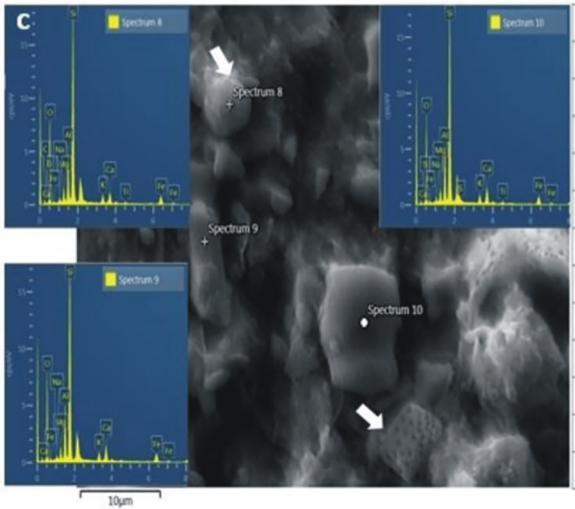

EDX ANALYSIS			
Element analysis	Spectrum 8	Spectrum 9	Spectrum 10
Mg	1.91 %	2.10 %	2.04 %
O	50.10 %	52.83 %	52.53 %
Al	5.84 %	7.19 %	7.21 %
Si	21.59 %	26.32 %	25.11 %
K	1.50 %	1.88 %	1.91 %
Fe	4.36 %	5.30 %	4.96 %
Ca	2.25 %	3.52 %	3.80 %
Na	0.99 %	0.87 %	1.32 %
Ti	0.41 %	----	0.60 %
C	11.05 %	----	---
S	----	----	0.54 %

Figure 2

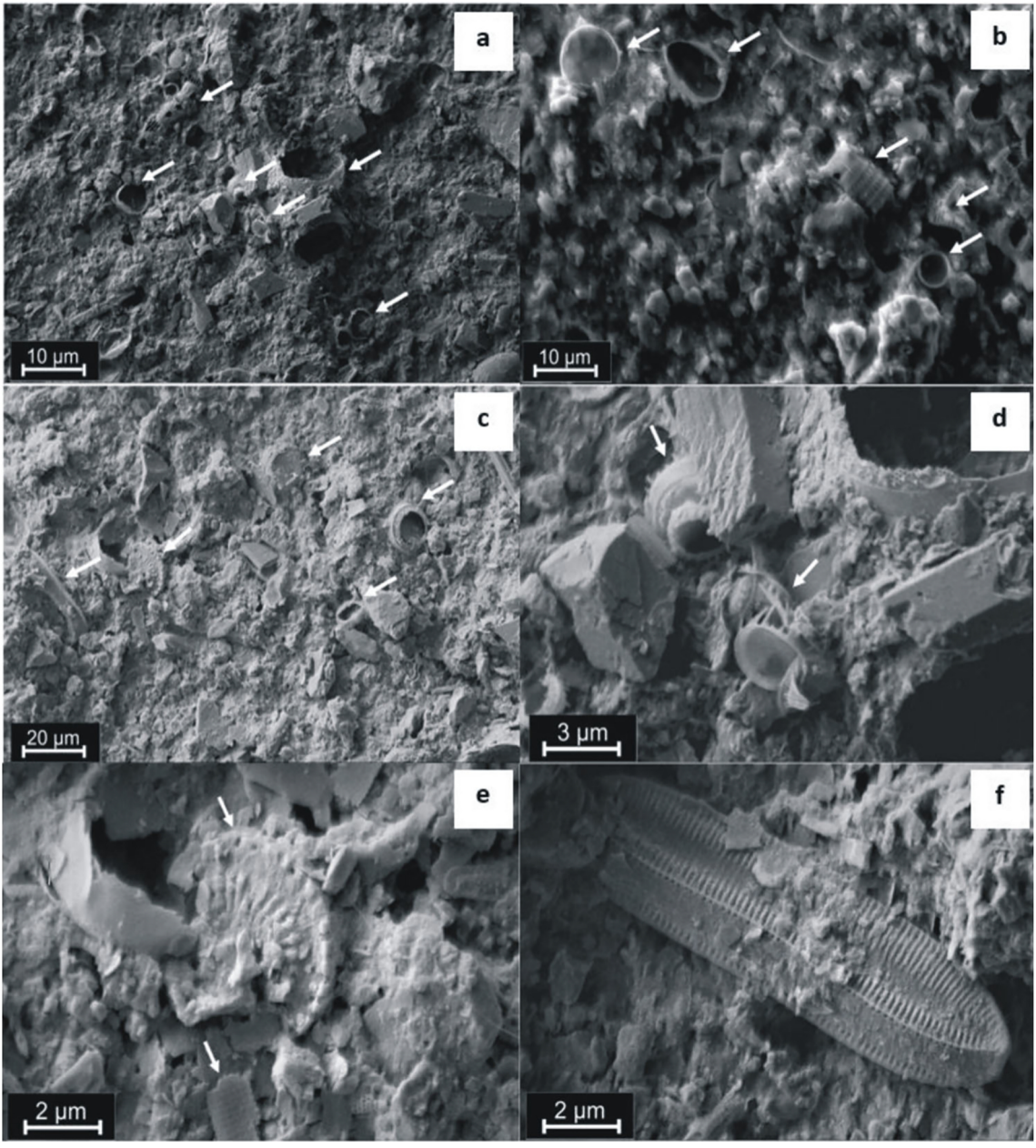

Figure 3

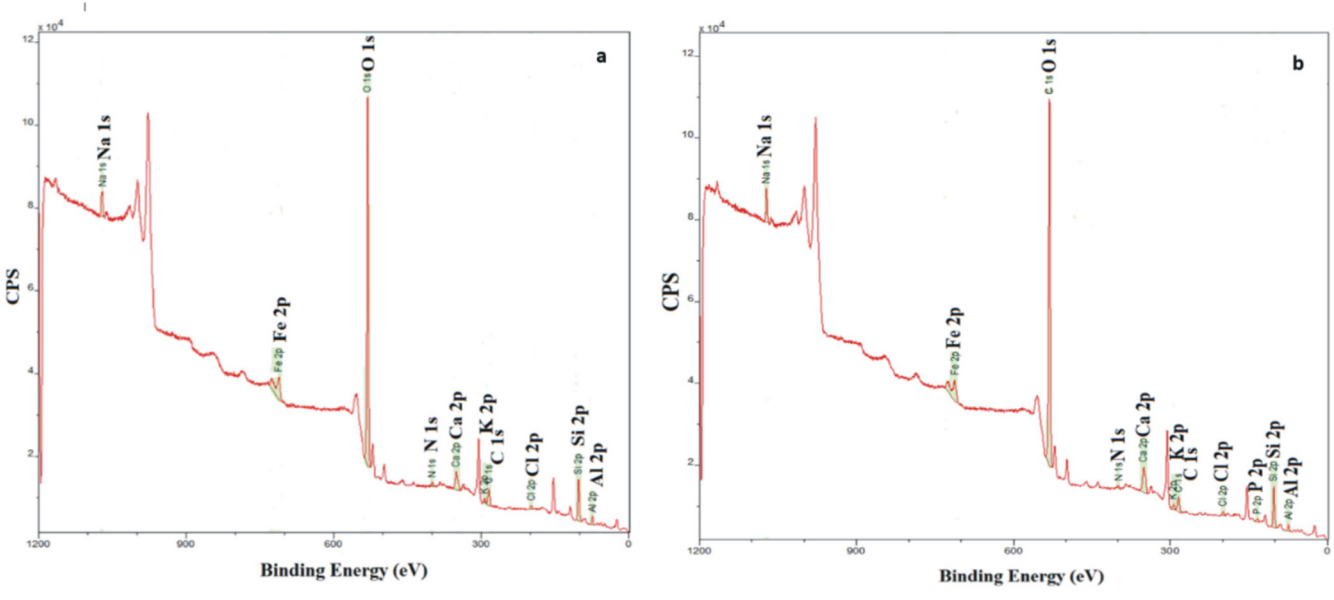
a
b
CPS
Binding Energy (eV)
Na 1s
O 1s
Fe 2p
N 1s
Ca 2p
K 2p
C 1s
Cl 2p
Si 2p
Al 2p
P 2p

Figure 4

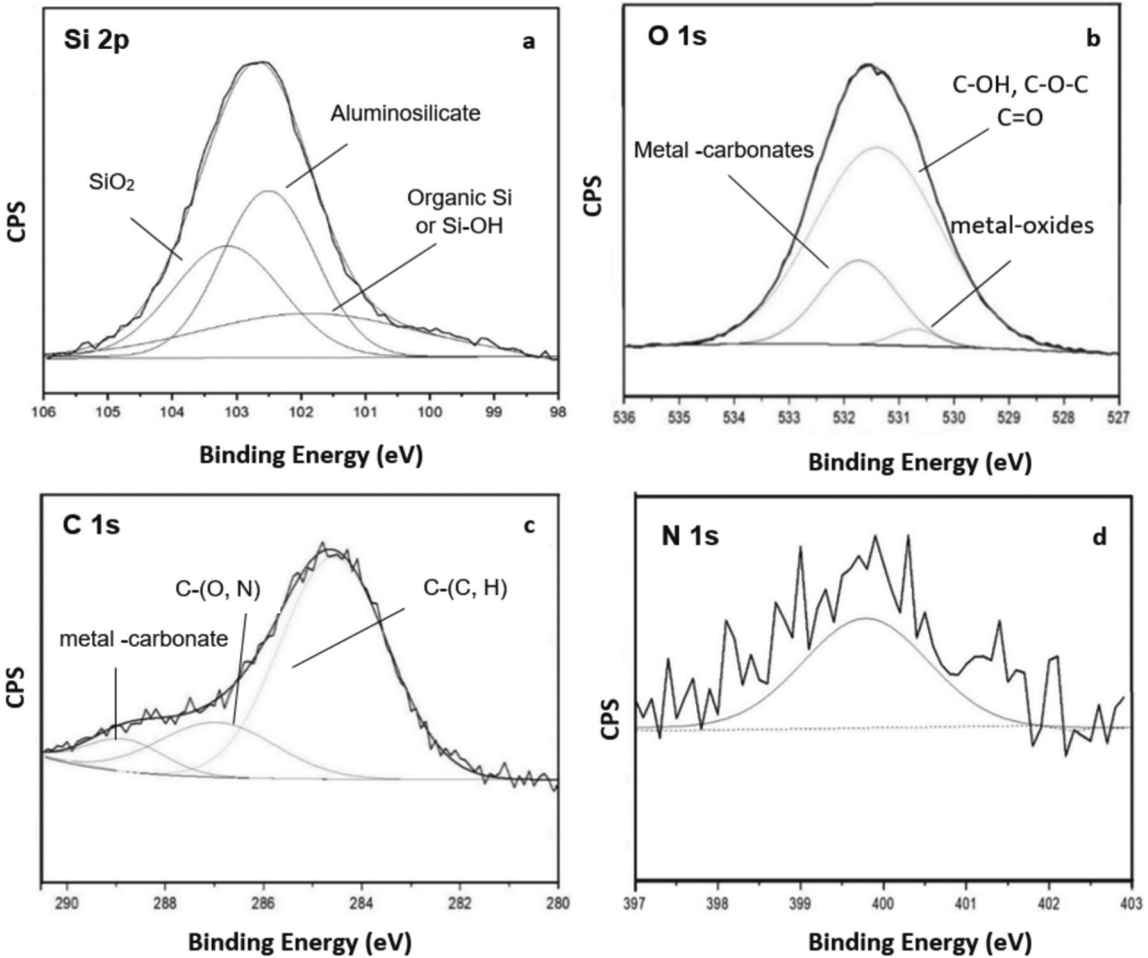
Si 2p
a
Aluminosilicate
SiO2
Organic Si
or Si-OH
CPS
106 105 104 103 102 101 100 99 98
Binding Energy (eV)
O 1s
b
C-OH, C-O-C
C=O
Metal -carbonates
metal-oxides
CPS
536 535 534 533 532 531 530 529 528 527
Binding Energy (eV)
C 1s
c
C-(O, N)
C-(C, H)
metal -carbonate
CPS
290 288 286 284 282 280
Binding Energy (eV)
N 1s
d
CPS
397 398 399 400 401 402 403
Binding Energy (eV)

Figure 5

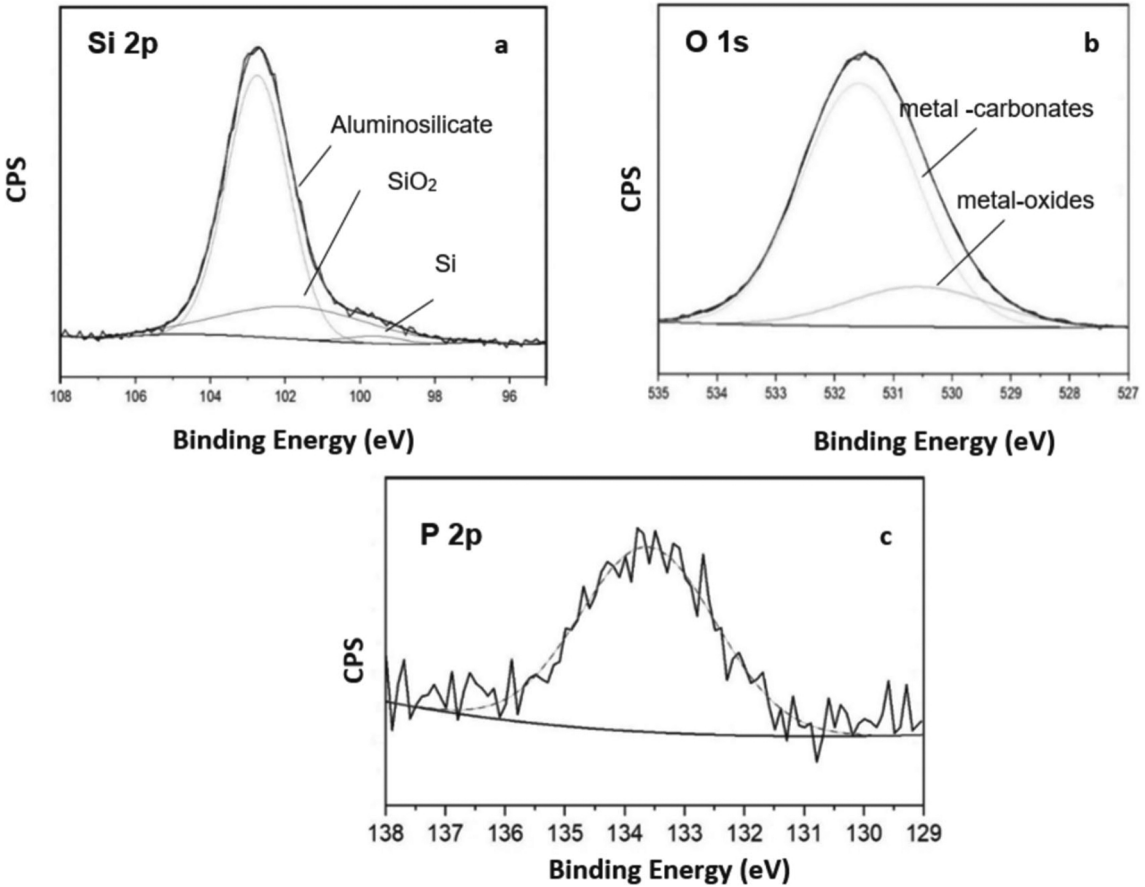
Si 2p
a
Aluminosilicate
SiO2
Si
CPS
108 106 104 102 100 98 96
Binding Energy (eV)
O 1s
b
metal -carbonates
metal-oxides
CPS
535 534 533 532 531 530 529 528 527
Binding Energy (eV)
P 2p
c
CPS
138 137 136 135 134 133 132 131 130 129
Binding Energy (eV)

Figure 6

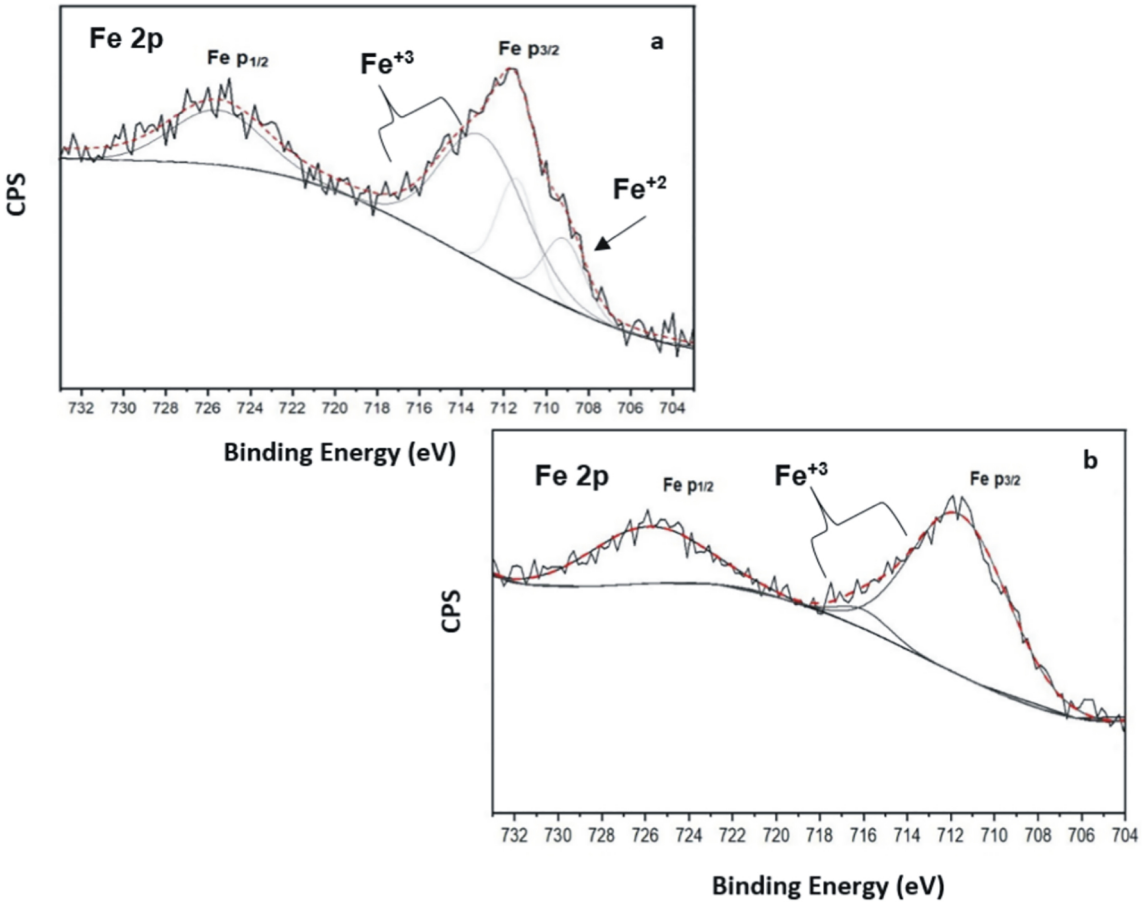
Fe 2p
Fe p1/2
Fe+3
Fe p3/2
a
Fe+2
CPS
732 730 728 726 724 722 720 718 716 714 712 710 708 706 704
Binding Energy (eV)
Fe 2p
Fe p1/2
Fe+3
Fe p3/2
b
CPS
732 730 728 726 724 722 720 718 716 714 712 710 708 706 704
Binding Energy (eV)

Figure 7

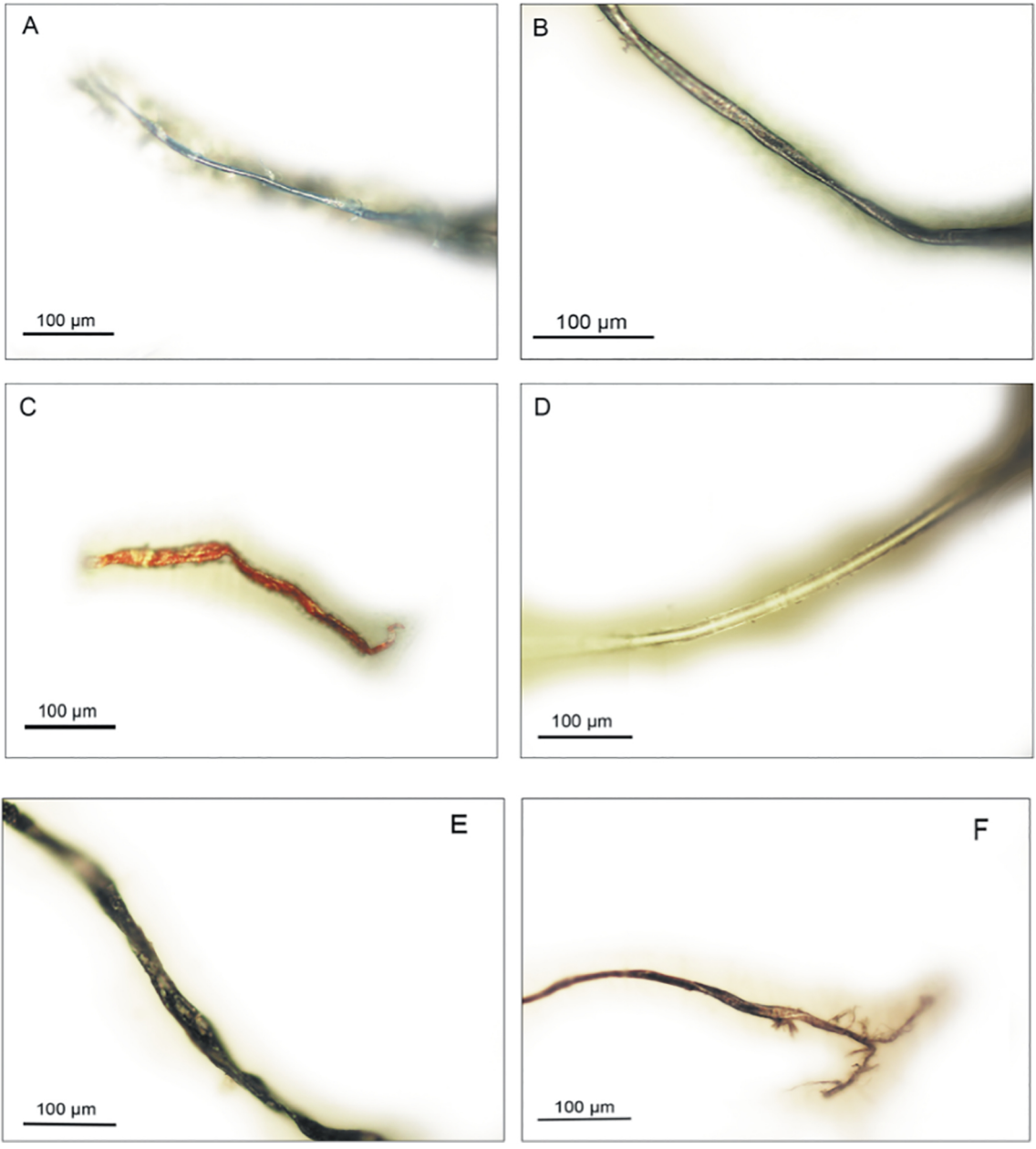

Figure 8

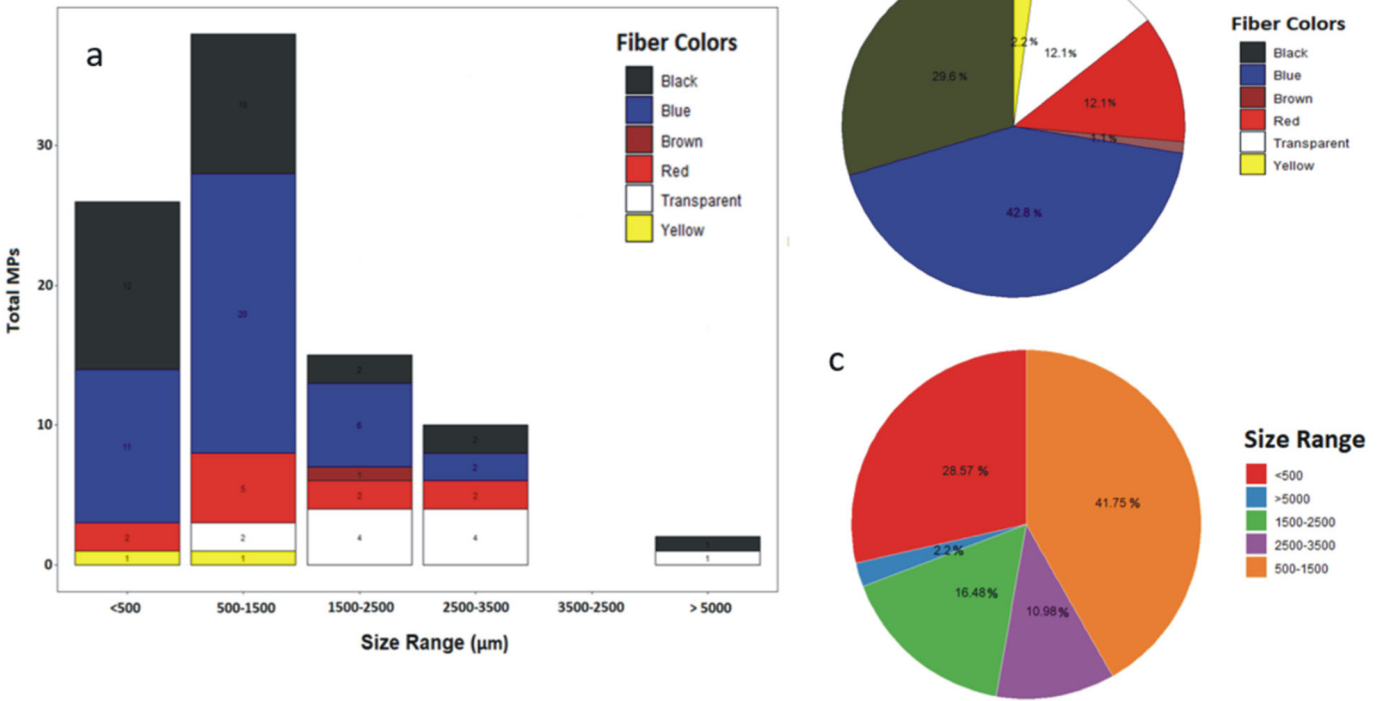
a
Fiber Colors
Black
Blue
Brown
Red
Transparent
Yellow
Total MPs
0
10
20
30
<500
500-1500
1500-2500
2500-3500
3500-2500
> 5000
Size Range (µm)
b
29.6 %
2.2%
12.1%
12.1%
1.1%
42.8 %
Fiber Colors
Black
Blue
Brown
Red
Transparent
Yellow
c
28.57 %
41.75 %
2.2 %
16.48%
10.98%
Size Range
<500
>5000
1500-2500
2500-3500
500-1500

Figure 9

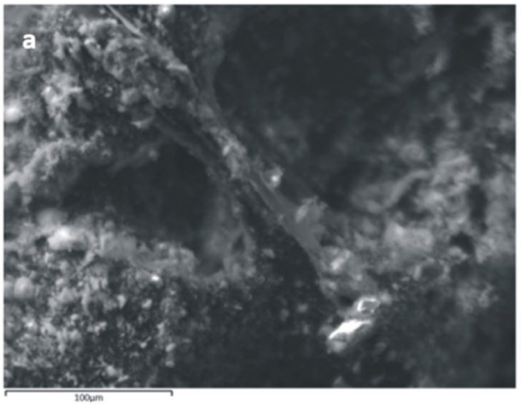

a2

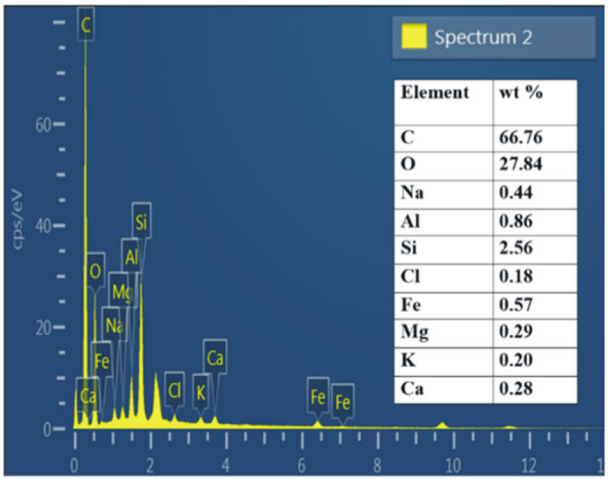

Element	wt %
C	66.76
O	27.84
Na	0.44
Al	0.86
Si	2.56
Cl	0.18
Fe	0.57
Mg	0.29
K	0.20
Ca	0.28

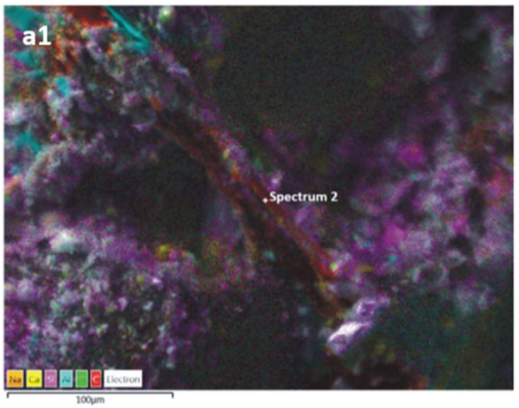

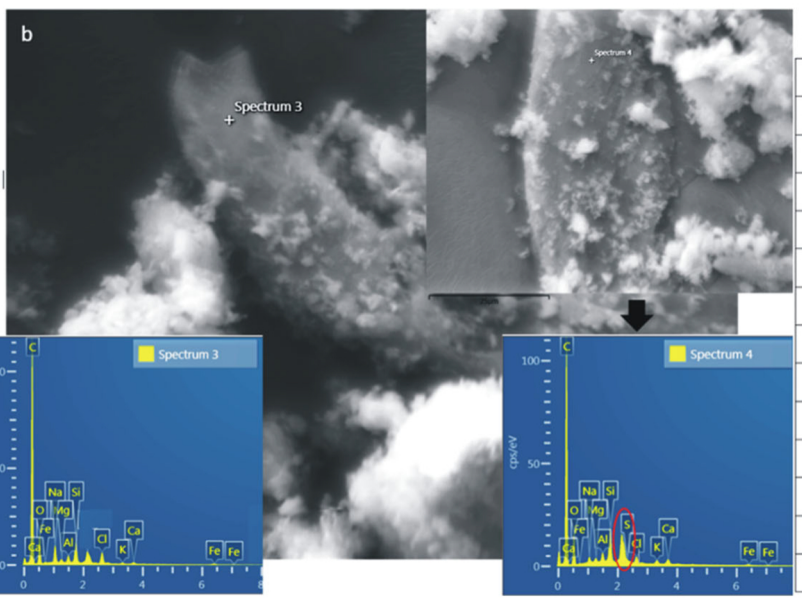

b1

EDX ANALYSIS		
Element analysis	Spectrum 3	Spectrum 4
Mg	0.17 %	0.21 %
O	18.64 %	19.19 %
Al	0.33 %	0.42 %
Si	0.96 %	1.45 %
K	0.09 %	0.28 %
Fe	0.20 %	0.18 %
Ca	0.15 %	0.43 %
Na	----	0.41 %
Ti	0.41 %	----
C	77.33 %	76.85 %
S	----	0.18 %
Cl	0.72 %	0.41 %

Figure 10

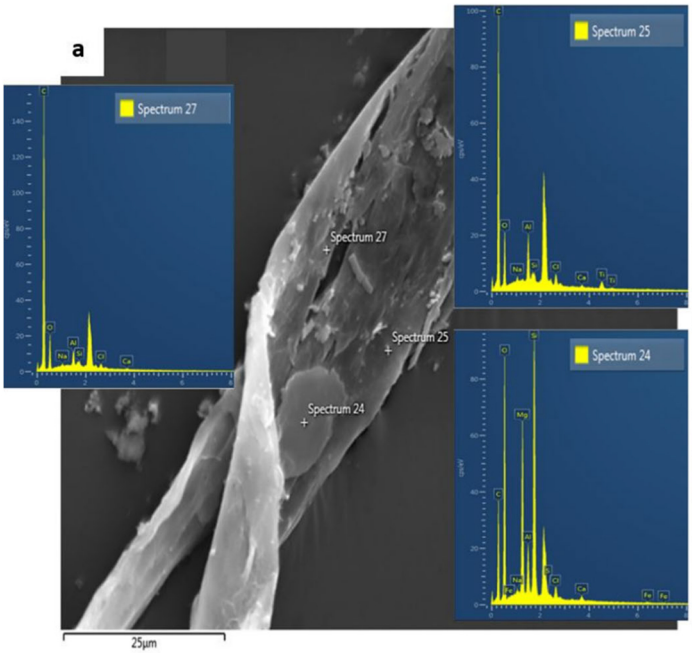

a1

EDX ANALYSIS			
Element analysis	Spectrum 24	Spectrum 25	Spectrum 27
Mg	6.45 %	----	----
O	44.02 %	25.19 %	20.66 %
Al	1.68 %	2.06 %	0.89 %
Si	8.4 %	0.3 %	0.22 %
Fe	0.13 %	----	----
Ca	0.25 %	0.18 %	0.07 %
Na	0.17 %	0.36 %	0.04 %
Ti	----	0.57 %	----
C	38.16 %	70.31 %	77.56 %
S	0.16 %	----	----
Cl	----	0.73 %	0.38%

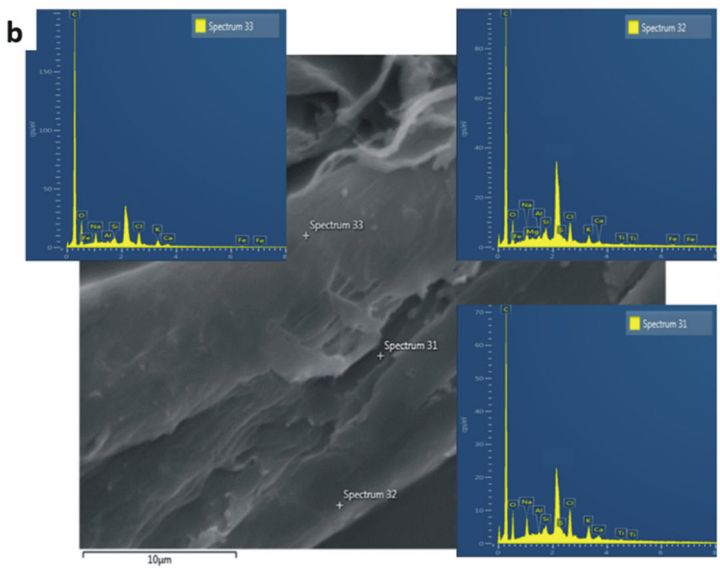

b1

EDX ANALYSIS			
Element analysis	Spectrum 31	Spectrum 32	Spectrum 33
Mg	----	0.09 %	----
O	15.01%	14.45 %	15.85 %
Al	0.12 %	0.18 %	0.12 %
Si	0.35 %	0.49 %	0.29 %
K	0.66 %	0.69 %	0.57 %
Fe	----	0.17 %	0.11 %
Ca	0.34 %	0.30 %	0.17 %
Na	1.41 %	1.07 %	0.98 %
Ti	0.14 %	0.14 %	----
C	79.29 %	80.72 %	80.87 %
S	----	0.3 %	----
Cl	1.89 %	1.42 %	1.04%

Figure 11

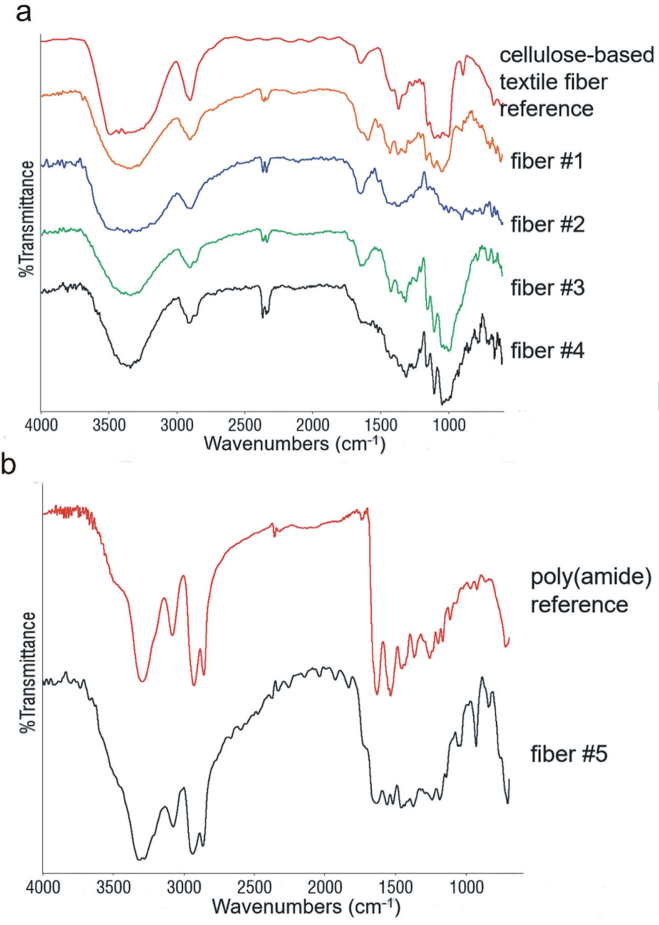
a
cellulose-based textile fiber reference
fiber #1
fiber #2
fiber #3
fiber #4
%Transmittance
4000 3500 3000 2500 2000 1500 1000
Wavenumbers (cm-1)
b
poly(amide) reference
fiber #5
%Transmittance
4000 3500 3000 2500 2000 1500 1000
Wavenumbers (cm-1)

Figure 12